

Parameterization and Modelling of Large Off-Road Tyres for Ride

Analyses

Part 1 - Obtaining Parameterization Data

M. Joachim Stallmann & P. Schalk Els* & Carl M. Bekker

Department of Mechanical and Aeronautical Engineering,

University of Pretoria, co Lynnwood Road and Roper Street,

Pretoria, 0002, South Africa

* Corresponding author.

E-mail address: schalk.els@up.ac.za

Telephone: +27 12 420 2045

E-mail address:

joachim@stallmann.co.za (M. Joachim Stallmann)

schalk.els@up.ac.za (P. Schalk Els)

carl.becker@up.ac.za (Carl M. Bekker)

Highlights

- Most tyre models rely on experimental test data.
- Obtaining parameterisation test data for large off-road tyres is challenging.
- A method of obtaining parameterisation and validation test data is proposed.
- A full set of measurement results are presented.

1 Abstract

Multi-body vehicle dynamic simulations play a significant role in the design and development process of off-road vehicles. These simulations require tyre models to describe the forces and moments, which are generated in the tyre-road contact patch, that act on the vehicle. All external forces acting on the vehicle are generated in the tyre-road interface or are due to aerodynamic effects. At the typical speeds encountered during off-road driving, aerodynamic forces can be neglected. The accuracy of the tyre model describing the forces in the tyre-road interface is thus of exceptional importance. It ensures that the simulation model is an accurate representation of the actual vehicle.

Various approaches are adopted when developing mathematical tyre models. The complexity of different mathematical tyre models varies greatly, as do the parameterisation efforts required to obtain the model parameters. The parameterization of most tyre models relies on some experimental test data that is used to extract the necessary information to fit model parameters. Acquiring the test data, with sufficient accuracy, is often the biggest challenge in the parameterisation process. Historically passenger car tyres have been the focal point for tyre model development. Larger tyres introduce some difficulties due to their size and load rating. Large off-road tyres, typically used in the construction, agriculture or military environment, cannot be tested on conventional tyre test rigs due to size and load ratings, meaning that different test approaches are required. Off-road truck tyres also differ in their construction which influences the force and moment generation of the tyre, meaning that tyre models that work well for passenger car tyres on relatively smooth, hard roads, don't necessarily give satisfactory results over rough off-road terrain. Research efforts are therefore increasing to meet the need of tyre models that can describe the behaviour of large off-road tyres over uneven terrain with sufficient accuracy.

In this paper different methods to acquire the required parameterization data of large off road tyres are discussed. Experimental measurements are conducted on a 16.00R20 Michelin XZL tyre. Laboratory tests, as well as field tests, over discrete obstacles and uneven hard surfaces were conducted. Published data for large off-road tyres is virtually non-existent. This paper presents an extensive set of parameterization and validation test data on a large off-road tyre that can be used by researchers to develop and validate tyre models.

Keywords:

Test data, parameterization, modal analyses, cleat, field test, test trailer, tyre model

2 Introduction to Tyre Testing

Mathematical vehicle dynamics models are often used to aid in the development of new vehicles. These models are only useful if they can reflect reality with sufficient accuracy. The modelling of the

tyre road interaction is of special importance as it influences the accuracy of the entire vehicle dynamics model. It can be said that a sufficiently accurate description of the tyre and the road is one of the most important aspects of creating a useful simulation model. All other components of the model are influenced by the forces and moments developed in the tyre contact patch. To create a balanced model the accuracy of the vehicle model should stand in a reasonable relationship to the applied vehicle-road contact model.

A wide range of tyre models and tyre contact models have been developed over the years [1]. Many of these models were developed for simulations that investigate handling manoeuvres of passenger cars, over smooth, hard man-made roads.

Researchers have developed and validated various tyre models to be used in simulations over uneven terrain [2]. Research has shown that physical tyre models can accurately predict tyre forces. These models however require excessive computer resources and calculation times. These limitations restrict their use in vehicle dynamic simulations. More compact models, such as empirical models, are much faster and require manageable computational power. Empirical models however struggle to represent the complex tyre behaviour [3].

The majority of the existing tyre models require experimental data during the parameterization process. The test data is used to extract parameters that define the tyre behaviour. The selection of the tyre model, to be used in a vehicle dynamic simulation, is thus often dependent on the availability of the required parameterization data. If the required test data cannot be obtained the model becomes obsolete.

Various techniques have been developed to obtain the required parameterization data. These techniques range from static stiffness test to in situ tyre tests. Some of the most popular test techniques are discussed in this section. The advantages and the shortcoming of the various test methods will be discussed shortly.

Static tests are performed on a non-rolling tyre. The investigations include tests to determine the shape and dimensions, stationary load deflection behaviour, footprint dimensions and modal

properties of the tyre. The advantages of these tests are that the test parameters and the environmental variables can be accurately controlled. These tests are also economically efficient. The short coming of the test method is that it describes the non-rolling tyre properties. The operation condition of interest, of the tyre, is however the rolling state.

To obtain the required parameterization data from rolling tyres, drum test rigs or flat track tyre test rigs are often used. The drum test rig simulates the road surface via a drum. Drum test stands typically have diameters from 2m to 5m. The drum surface can either be steel or coated with a “safety walk” coating to improve the friction conditions [4]. Modern drum tests allow caskets to be mounted on or in the drum. These caskets are filled with real pavements to simulate real road driving conditions [5]. These drum tests are generally developed to test passenger car tyres and thus often have a maximum track width of 400mm and support a maximum tyre loads of up to 50kN [6]. Tyres can be tested on drums at velocities greater than 250km/h. Drum test results are often used as parameterization data for tyre models but are more appropriately used for ranking analysis or for investigations in to the relative effect of load, speed and temperature changes on the tyre behaviour. The use of the test data is limited due to the curved contact between the tyre and the test surface as well as the difficulty in achieving a test surface representative of real road surfaces. The unnatural curvature affects the tyre behaviour and influences the generated force and moment components of the tyre. To circumvent this short coming, tyre model parameterization software is being developed in such a way so as to consider the road curvature effects.

To eliminate the curved contact patch of the drum test method, flat track tire test machines are used. These tyre test stands simulate the road surface as an endless belt. The belt that simulates the road is supported by two drums and is coated with an abrasive surface coating [7]. The coating increases the friction when compared to the uncoated steel belt, however it is not identical to an actual road surface. The flat track test rig can only be used to test tyre behaviour over a flat belt and can thus not be used to perform cleat tests or be used to excite the tyre in the normal direction.

To perform laboratory cleat tests on a flat surface a flat plank tyre test rig can be used. The flat plank, simulating the road surface, is generally less than 5m long, and can move in the longitudinal direction. Cleats are mounted onto the flat surface to conduct tyre enveloping behaviour tests. The disadvantage of this test rig is that tests can only be conducted at speeds of less than 0.2km/h [8].

Outdoor tests, also known as field tests, are generally conducted using trucks or test trailers. These trucks and trailers are equipped with a special hub on which the test tyre is mounted. The on-road tyre test rig, developed by TNO, is used to test passenger car tyres, motorcycle tyres and light truck tyres up to a maximum speed of 150km/h at a maximum normal load of 10kN [9]. Test trailers have also been developed to test large truck tyres. The single axle test trailer, used by the University of Pretoria [10], comprises of two core structures, the mainframe and the sub frame. The test tyre is mounted to the sub frame. The sub frame is in turn connected to mainframe by six load cells positioned to allow the forces and moments acting on the wheel to be calculated. The trailer can be loaded with weights so that the static load on the tyre ranges from 2400kg to 5200kg.

The advantage of outdoor testing is that the tests can be conducted under real operating conditions. Tests on arbitrary road surfaces such as asphalt or concrete are possible, as are tests under different environmental conditions including ice or rain. The disadvantages of these tests are that they are quite cumbersome and more difficult to control.

3 Experimental Setup and Results

The tyre that was analysed for this project was the Michelin XZL 16.0R20 all-terrain tyre. The tyre can be used for on or off-road terrain. The tyre was designed with a self-cleaning, open shoulder tread design with offset elements to increase traction on various terrains such as snow, sand or mud.

A full width steel belt and an elastic protector ply help to protect the tyre against off-road hazards. The tyre could be used with or without a tube. The tyre is rated for a maximum speed of 88km/h and a maximum load of 6595kg. The inflated diameter and width were established to be 1340mm and

460mm respectively. The total mass of the wheel, tyre and rim, was experimentally determined to be 240kg.

The tyre tests can be divided into static and dynamic tests. The tests are summarized in Fig.1. The first set of parameterization data was acquired in the laboratory. These tests were conducted on a non-rolling tyre. The second set of tests were field tests and were conducted using a test trailer. These tests were conducted to acquired parameterization data from a rolling tyre.

3.1 Non-rolling Tyre Tests

Tests on the non-rolling tyre include vertical stiffness on a flat surface as well as cleats, contact area, modal analyses and geometric parameters.

3.1.1 Vertical Tyre Stiffness

The vertical tyre force vs. vertical deflection is an important tyre characteristic. The experimental setup is shown in Fig. 2. The tests were done in the laboratory where the rim was fixed. A hydraulic actuator, positioned horizontally inline with the centre of the wheel, was used to compress the tyre. A large flat steel plate was used to simulate the road surface. During the test the applied load and the resulting tyre displacement was measured. To minimize the effect of elasticity in the test fixtures and floor, the tyre displacement was measured with a laser displacement instrument mounted between the rim and the flat steel plate. The tyre was tested at inflation pressures of 100kPa, 300kPa and 550kPa.

Figure 3 shows the relationship between the applied load and displacement. The 0.5Hz sinusoidal displacement input results in the hysteresis loop as shown. The measured data is clearly nonlinear, but a linear curve fit is shown for the three result sets.

Table 1 shows the average loads for every 10 mm displacement, to create a nonlinear force displacement curve. These curves describe the tyre behaviour better than the linear curve fit.

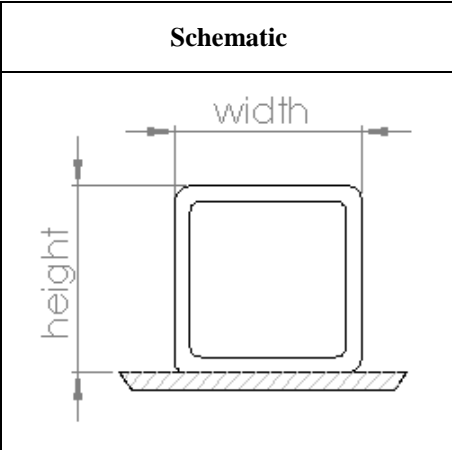
Table 1 Tyre load deflection data

Displacement [mm]	Applied load [N], 100kPa	Applied load [N], 300kPa	Applied load [N], 550kPa
0	0	0	0
-10	-1 905	-3 496	-6 354
-20	-4 716	-9 445	-15 537
-30	-7 221	-15 559	-25 250
-40	-9 947	-21 968	-36 872
-50	-13 415	-29 011	-48 446
-60	-17 673	-37 581	-62 502
-70	-21 582	-45 717	-74 730
-80	-25 616	-54 191	-88 151

3.1.2 Tyre Stiffness on Cleat

Cleats are discrete obstacles that are used in tyre characterization and parameterization tests. Square cleats are commonly used but other shapes are also available. To collect experimental data that describes the enveloping effects of a tyre, static cleat tests were conducted on square cleats. The test setup was similar to the setup used to determine the vertical tyre stiffness. Cleats with various dimensions were fitted to the flat plate. The tests were conducted with cleats orientated in the both lateral and longitudinal directions.

Table 2 Cleat dimensions

Schematic	Width [mm]	Height [mm]
	25.4	25.4
	38	38
	51	51
	76.3	76.3
	100	50

The dimensions of the cleats should be related to the expected tyre deflection under normal operating conditions. For a tyre where a large deflection was expected during normal operation, the cleats

should be larger than for a tyre with a smaller expected deflection. Five different cleat dimensions were investigated. Table 2 shows the dimensions of the cleats that were chosen for the tests. The length of the cleat was chosen so that it would extend beyond the tyre contact patch.

During the tests the applied force and the tyre displacement were measured. The origin of the displacement is defined as the point where the tyre first makes contact with the cleat. The tyre was tested at an inflation pressure of 100kPa, 300kPa and 550kPa.

Fig. 4 to Fig. 9 show the results of these tests, with cleats orientated in the longitudinal and lateral direction, at 100kPa, 300kPa and 550kPa tyre inflation, respectively. It can be seen that the expected tyre stiffness decreases for all static cleat tests. The tyre stiffness decreases more at lower inflation pressures and is more predominant with the laterally orientated cleat. Also note that the cleat causes certain deformation before the tyre starts contacting the flat plate again.

3.1.3 Tyre Contact Area

To determine the tyre contact patch dimensions, the tyre contact area test rig was used [11]. The test rig had a movable axle, on which the test tyre was mounted. It could be moved towards a bullet proof glass sheet using two hydraulic actuators. The contact between the glass and the tyre tread was visible on the opposite side of the glass. A calibrated camera was then used to capture the contact area. Fig.10 shows the captured image for the Michelin tyre at 500kPa at a normal load of 44.1kN. The red line in the image is used as reference and has a length of 100mm. The tyre contact patch dimensions as well as the enclosed area and the true area of contact are listed in Table 3.

Table 3 Tyre contact patch dimensions







		Load (kN)				
		39.2	44.1	49.1	54.0	58.9
100kPa	Length (mm)	642	686	728	732	739
	Width (mm)	372	370	370	361	360
	Contact area (m ²)	0.104	0.111	0.121	0.124	0.124
	Enclosed area (m ²)	0.226	0.237	0.256	0.254	0.258
300kPa	Length (mm)	445	476	469	499	522
	Width (mm)	366	366	371	375	373
	Contact area (m ²)	0.073	0.077	0.087	0.088	0.073
	Enclosed area (m ²)	0.161	0.161	0.172	0.179	0.161
500kPa	Length (mm)	372	377	-	405	425
	Width (mm)	364	370	-	371	372
	Contact area (m ²)	0.054	0.059	-	0.067	0.07
	Enclosed area (m ²)	0.116	0.122	-	0.139	0.147

3.1.4 Tyre Modal Analyses

A modal analysis was conducted with the use of a Polytec PSV-400 Scanning Laser Vibrometer as shown in Fig.11. These tests were conducted to determine the frequencies of the first few vibration modes of the tyre. The tests were conducted in the lateral and longitudinal scanning surface direction. They were conducted at different impulse amplitudes to determine the linearity of the tyre at different loads.

Table 4 shows the modal analysis results for an impulse load of 40kN and at tyre pressures of 100kPa, 300kPa and 550kPa. The vibration mode shapes are organized according to Gipser [12]. The first

Table 4 Tyre modal analysis results

FTire Vibration mode	Vibration mode illustration	Description	Frequency [Hz], 100kPa	Damping [%], 100kPa	Frequency [Hz], 300kPa	Damping [%], 300kPa	Frequency [Hz], 550kPa	Damping [%], 550kPa
1		natural frequency of the in-plane 'rigid-body' rotation about wheel spin axis	-	-	-	-	-	-
2		natural frequency of the 'rigid-body' movement in longitudinal or vertical direction	15.18	2.61	22.72	2.94	33.51	2.01
3		natural frequency of the 'rigid-body' movement in lateral direction	12.22	2.6	16.88	2.33	20.09	2.19
4		natural frequency of the out-of-plane 'rigid-body' rotation about any axis perpendicular to wheel spin axis	33.11	4.52	29.99	1.19	17.00	1.44
5		third natural frequency of the in plane body movement	46.24	0.19	52.39	0.54	53.77	0.06
6		third natural frequency of the out of plane body movement	53.98	0.19	43.39	0.67	45.93	0.13

mode shape represented the natural frequency of the in-plane ‘rigid-body’ rotation about wheel spin axis. This vibration mode could not be determined with the current test setup as the measurements were taken perpendicular to the side wall and to the contact patch of the tyre.

3.1.5 Other Parameters

The weight of the tyre is 154kg and the complete wheel, including the carcass, run flat insert and rim, were weighed at 240kg. The tread rubber stiffness was determined experimentally and was found to have a ShoreA hardness value of 60.

The outer contour of the test tyre was measured to describe the unloaded carcass shape. Multiple measurements were taken to determine the outer profile of the tyre as the tyre had an irregular tread pattern. Figure 12 shows the result of two tread carcass sections and the tyre sidewall. The figure depicts the relationship between the section height and the tread width. Tyre outer contour dimensions are given in Table 5. The origin of the measurements was defined on the left side of the tread pattern. The tests were conducted at an inflation pressure of 300kPa.

Table 5 Tyre outer contour dimensions

Tread width(mm)	Section height(mm)	Tread width(mm)	Section height(mm)
-30	163.3	210	0.0
0	48.4	240	0.0
30	19.1	270	0.2
60	8.3	300	2.2
90	3.8	330	5.6
120	1.4	360	10.2
150	0.0	390	26.4
180	0.0	420	103.5

3.2 Dynamic Tyre Tests

The acquisition of the required dynamic parameterization data, for large off road tyres, presents a challenge for conventional test methods. These conventional methods make use of either a roller drum test rig or a flat track test rig. They are limited to passenger cars and light truck tyres. The maximum

loads of many test rigs are limited to less than 50 000N. The Michelin XZL 16.00R20 used in this study has a maximum static load rating of 65 000N.

The second limitation is the dimensions of the test rigs. Commercial test rigs have a width of about 400 mm while the overall width of this tyre is about 435 mm. The relationship between the drum diameter and the tyre diameter is also decreased which results in an inaccurate representation of the contact patch.

To eliminate these limitations a tyre test trailer was used to acquire the experimental data. The experimental setup used for these tests is shown in Fig. 13. The test setup comprised of a large towing vehicle and the tyre test trailer. The trailer consists of a main frame and a sub frame. The trailer can be loaded with weights so that the static load on the tyre ranges between 2400kg and 5200kg. The wheel, with the tyre that needed to be tested, was mounted to the sub frame on the right hand side of Fig 13.

The sub frame is connected to the mainframe by six load cells that are positioned to enable all the forces and moments acting on the wheel to be measured. Since the tyre test trailer has no suspension, all the forces acting on the load cells, connecting the main frame to the sub frame, could be related to the forces that are generated in the tyre contact patch. The wheel hubs, of the tyre test rig, can be adjusted to change the slip angle of the tyre. The slip angle can be adjusted between -2 degrees and 10 degrees. The yaw angle of the test trailer is not controlled. The slip angle of the tyre is measured using a Correvit non-contact optical slip sensor [13].

The position of the centre of mass and the moments of inertia of the test trailer, without the tyres and rims fitted, were determined experimentally. The CAD model is shown in Fig. 14. The pitch moment of inertia was determined to be 58594kgm^2 , while the roll and yaw moments of inertia were determined as 3776kgm^2 and 8958kgm^2 respectively. The moments of inertia are calculated around the centre of gravity of the trailer. The dimensions of the tyre test rig are listed in Table 6. All co-ordinates are referenced from the tow hitch.

Table 6 Tyre tester dimensions

	X (mm)	Y (mm)	Z (mm)
Center of mass	-2847	-5	-471
Left Wheel attachment	-3163	1538	-508
Right wheel attachment	-3160	-1512	-508
Left Kingpin	-3163	962	-508
Right Kingpin	-3160	-945	-508

The tyre track width of the trailer was wider than the track width of the towing vehicle. This allowed the towing vehicle to avoid obstacles while the test trailer was towed over these obstacles. Due to the different track widths the test trailer was excited by the tyres of the trailer as they clear the obstacles while it was supported only by the towing hitch.

3.2.1 Tyre Damping

To determine the damping coefficient of the non-rolling tyres, the tyre test trailer was lifted until the wheels just lost contact with the ground. The trailer was then dropped. The vertical displacement of the rim was measured until the test trailer oscillations damped out and the trailer reached its static equilibrium again. Figure 15 shows the tyre displacements that were measured during the drop test.

To calculate the damping coefficient of the tyre, it was assumed that the hitch of the towing vehicle was fixed and unable to move during the drop test. The test trailer could then be approximated as a pendulum connected to the ground by a spring and a damper on the one side, and pivoting about the hitch on the other end.

For small rotational displacements the small angle assumption could be made, so that $\sin\theta = \theta$ and $\cos\theta = 1$. The equation of motion of the pendulum is then given by:

$$I_0\ddot{\theta} + cl^2\dot{\theta} + kl\theta = 0 \quad (1)$$

Where I_0 is the moment of Inertia of the trailer about the axis of rotation, c the damping coefficient and k the tyre stiffness. The variable l is the distance between the tow hitch and the wheels. The equations can be simplified to:

$$\ddot{\theta} + \frac{cl^2}{I_0}\dot{\theta} + \frac{kl}{I_0}\theta = 0 \quad (2)$$

and written in the standard form:

$$\ddot{\theta} + 2\xi\omega_n\dot{\theta} + \omega_n^2\theta = 0 \quad (3)$$

The undamped natural frequency can then be defined as:

$$\omega_n = \sqrt{\frac{kl^2}{I_0}} \quad (4)$$

The damping ratio was then given by:

$$\xi = \frac{cl^2}{2\omega_n I_0} \quad (5)$$

From the measured data the logarithmic decrement of the displacement amplitudes of two consecutive oscillations could be calculated using:

$$\delta = \ln \frac{x_1}{x_2} \quad (6)$$

The damping ratio could then be calculated using:

$$\xi = \frac{\delta}{\sqrt{\delta^2 + (2\pi)^2}} \quad (7)$$

The damping coefficient, c , could then be calculated for the test tyre. Using this procedure the average non-rolling dynamic damping coefficient for the Michelin 16.00R20 tyre was calculated as 2.66Ns/mm. Note that the damping behaviour of a tyre is highly nonlinear as it depends on the viscoelastic damping behaviour of the rubber and the energy dissipation due to the interaction between the tyre and the road. A linear approximation is made here as many tyre models describe the tyre damping using a linear relationship.

3.2.2 Dynamic Cleat Tests

For the dynamic cleat test the trailer was pulled over square cleats of various sizes. Two orientations were investigated, perpendicular to the direction of travel and at a 45 degree angle. The dimensions, width by height, of the cleats that were investigated were:

- 38mm x 38mm
- 50mm x 50mm
- 76.3mm x 76.3mm
- 100mm x 100mm

Three different load cases, with a wheel load of 2375kg, 3895kg and 5095kg respectively, were investigated. The load cases represented 36%, 59%, and 77% of the maximum rated wheel load, load index (LI). The dynamic cleat tests were conducted at three test velocities of 10 km/h, 20km/h and 30km/h respectively.

Figure 16 shows the results of a dynamic cleat test. The tyre test trailer was towed at a speed of 10 km/h over a 76.3 mm cleat, orientated perpendicular to the direction of travel.

The test trailer was loaded to 59% of the LI of the tyres. The top left image shows the tyre approaching the cleat. The normal force, longitudinal force and rolling moment are also shown in the figure. The vertical green line represents the instant at which the photo was taken. The dynamic tyre damping, using the method as described in section 3.2.1, for this test was determined as 3.25Ns/mm.

Figure 17 depicts the results of a 50mm cleat test where the cleat was orientated at a 45 degree angle. The tyre tester was towed at a speed of 10 km/h over the obstacle and was not loaded with any additional weight, thus representing 36% of the LI. Due to the 45 degree orientation of the obstacle a lateral force is generated in the contact patch.

The tests were performed several times to ensure that the results were repeatable. The results correlated extremely well amongst the different measurements taken. Figure 18 shows two different cleat test runs, at 20 km/h, to illustrate the repeatability of the cleat tests. Cleat test where the cleats are orientated at an angle did not show the same agreement. The differences in the measurement can be linked to the difficulty of consistently positioning the test trailer in the middle of the test track.

3.2.3 Handling Tests

The lateral tyre characteristics of the tyre were also investigated. Side force vs. slip angle characteristics, extracted from data recorded when towing the test trailer at constant speed in a straight

line, are indicated in Fig. 19 for three vertical loads. The corresponding self-aligning moment vs. slip angle behaviour, for three different load cases, of the tyre is shown in Fig. 20.

3.2.4 Validation Tests

The second set of field tests were conducted to be used as validation data. Validation data would not be used in the parameterization process of the tyre. Tests that were conducted for validation purposes were:

- Trapezoidal bump
- Belgian paving
- Fatigue track
- Parallel corrugations track
- Angled corrugations track

The trapezoidal bumps are steel bumps with known dimensions. During the trapezoidal tests the tyre test rig was towed over the obstacle while the towing vehicle avoided the obstacles. Fig. 21 depicts the dimensions of the trapezoidal bumps that were used during the tests.

Fig. 22 shows the results of a trapezoidal obstacle test conducted at speed of 4km/h. The trailer is loaded to 59% of the LI.

The remaining validation tests were conducted on various test tracks at the Gerotek Test Facilities [11]. The test tracks have a length of one hundred meters and a width of four meters. The three dimensional road profiles were measured using a mechanical profilometer [14]. The measured road profiles allow an accurate road representation during simulations. The right tyre was mounted to the sub frame of the tyre tester. During the test it was on the test track while the left wheel and the towing vehicle were rolling on a smooth concrete surface.

The Belgian paving, also known as the Belgian block road, is often used to test the durability and ride comfort of vehicles. The blocks on the track had a random width but a regular length of 134 mm perpendicular to the direction of travel.

Figure 23 shows the measured forces and moments that are generated in the test tyre contact patch during a validation test on the Belgian paving, at a speed of 5km/h with no extra weight loaded on to the test trailer.

These validation test results will be used in Part 2 of the paper to quantify the accuracy of different tyre models parameterized using the data provided in this paper.

4 Conclusions

Laboratory tests were conducted on a non-rolling tyre. The static tyre stiffness was experimentally determined on a flat surface as well as square cleats, mounted in the lateral and longitudinal direction. The tyre carcass shape was measured and the footprint dimensions of the tyre were determined at various tyre inflation pressures and normal loads, using cleats with different dimensions. A modal analysis was also conducted to determine the vibration modes and natural frequencies of the tyre.

Dynamic cleat tests were also conducted to be used during the parameterization and validation process using a tyre test trailer. The repeatability of the parallel cleat tests was exceptionally good while the angled cleat tests did not show the same agreement. This was due to the difficulty found in positioning the test trailer exactly in the centre of the track to ensure that both wheels make contact with the cleats simultaneously.

Field tests were conducted over hard but rough terrains. These tests will be used in Part 2 of this paper to validate different mathematical tyre models. The field tests were conducted on various road surfaces found at the Gerotek Test Facilities. Tests were conducted on the Belgian block road, fatigue track, parallel and angled corrugations as well as discrete obstacles.

The extensive set of test data provided in this paper will be extremely useful to researchers that develop tyre models and fills the gap in the world of tyre data for large off-road tyres.

5 Notation

Symbol	Unit	Description
c	Ns/m	damping coefficient
I_0	kgm^2	moment of inertia about point
k	N/m	spring stiffness
l	m	pendulum length
x_1	m	amplitude of the first displacement oscillation
x_2	m	amplitude of the second displacement oscillation
$\dot{\theta}$	rad/s	rotation angular velocity
$\ddot{\theta}$	rad/s^2	rotation angular acceleration
ω_n	rad/s	undamped natural frequency
δ		logarithmic decrement
θ	rad	rotation angular displacement
ξ		damping ratio

6 References

- [1] Schmeitz, A.J.C., 2004. *A Semi-Empirical Three-Dimensional Model of the Pneumatic Tyre Rolling over Arbitrarily Uneven Road Surfaces*, PhD Thesis, Delft University of Technology, Delft, The Netherlands.
- [2] Zegelaar, P.W.A., 1998, *The dynamic response of tyres to brake torque variations and road unevenness*, PhD Thesis, Delft University of Technology, Delft, The Netherlands.
- [3] Frey, W.F., 2009, *Development of a rigid ring tire model and comparison among various tire models for ride comfort simulations*, Master's Thesis, Clemson University, August 2009.
- [4] Rill, G., 2006, *Vehicle Dynamics*, Lecture notes, Fachhochschule Regensburg, viewed 10 August 2013, from <https://hps.hs-regensburg.de/~rig39165/>.
- [5] Schwalbe, G., n.d., *TYROSAFE 1st workshop*, viewed 10 August 2013, from http://tyrosafe.fehrl.org/?m=49&mode=download&id_file=7796
- [6] TÜV SÜD., n.d., *Test Rigs for Tires/Wheels*, viewed 10 August 2013, from <http://www.tuev-sued.de/uploads/images/1263905646961806440579/Produktblatt-Test-Rigs-Tires--Wheels-englisch.pdf>

- [7] MTS., n.d., *Flat-Trac®Tire Test Systems*, viewed 10 August 2013, from http://www.mts.com/ucm/groups/public/documents/library/dev_002227.pdf
- [8] Cremens, R., 2005, *Investigating Dynamic Tyre Model Behavior*, Unpublished Master's Thesis, Eindhoven University of Technology.
- [9] De Roon, M., 2006, *Tire modeling for car, truck, motorcycle and heavy duty industrial applications using TNO Delft-Tyre*, Conference presentation, European LMS Conference, Munich, Germany
- [10] Stallmann, M.J., Els, P.S., 2013., *Data acquisition and parameterization procedure for large, off-road tires* , Proceedings of the 7th Americas Regional Conference of the International Society for Terrain-Vehicle Systems - Tampa, Florida, USA, November 4-7, 2013
- [11] Gerotek Test Facilities, n.d., viewed 2 July 2013, from www.gerotek.co.za.
- [12] Gipser, M., n.d., *The FTire Tire Model Family*. , viewed 2 July 2013, from <http://www.cosin.eu/literature>.
- [13] Correvit, n.d., Correvit non-contact optical sensor, viewed 13 August 2013, from http://www.corrsys-datron.com/optical_sensors.htm.
- [14] Bekker, C.M., Els, P.S., 2014., *Profiling of rough terrain* , International Journal of Vehicle Design, Vol. 64, Nos. 2/3/4, 2014

Figure captions

Figure 1 Experimental tyre test summary

Figure 2 Vertical tyre stiffness test setup

Figure 3 Static tyre deflection load curve

Figure 4 Longitudinal cleat - Load vs. Displacement curve, 100kPa

Figure 5 Longitudinal cleat - Load vs. Displacement curve, 300kPa

Figure 6 Longitudinal cleat - Load vs. Displacement curve, 550kPa

Figure 7 Lateral cleat - Load vs. Displacement curve, 100kPa

Figure 8 Lateral cleat - Load vs. Displacement curve, 300kPa

Figure 9 Lateral cleat - Load vs. Displacement curve, 550kPa

Figure 10 Tyre contact patch image, 500kPa, 44,1kN

Figure 11 Modal analysis test setup

Figure 12 Test tyre outer contour

Figure 13 Dynamic test setup

Figure 14 CAD model of tyre tester

Figure 15 Tyre test trailer drop test result

Figure 16 Cleat test measurement result, 76.3mm, 59% LI

Figure 17 Cleat test measurement result, 50mm oblique, 36% LI

Figure 18 Comparison of two 38mm Cleat test, 59% of LI

Figure 19 Side force vs slip angle

Figure 20 Self-Aligning moment vs slip angle

Figure 21 Trapezoidal bump dimensions

Figure 22 trapezoidal obstacle test, 59% of the LI

Figure 23 Belgian paving measurement, 36% of the LI

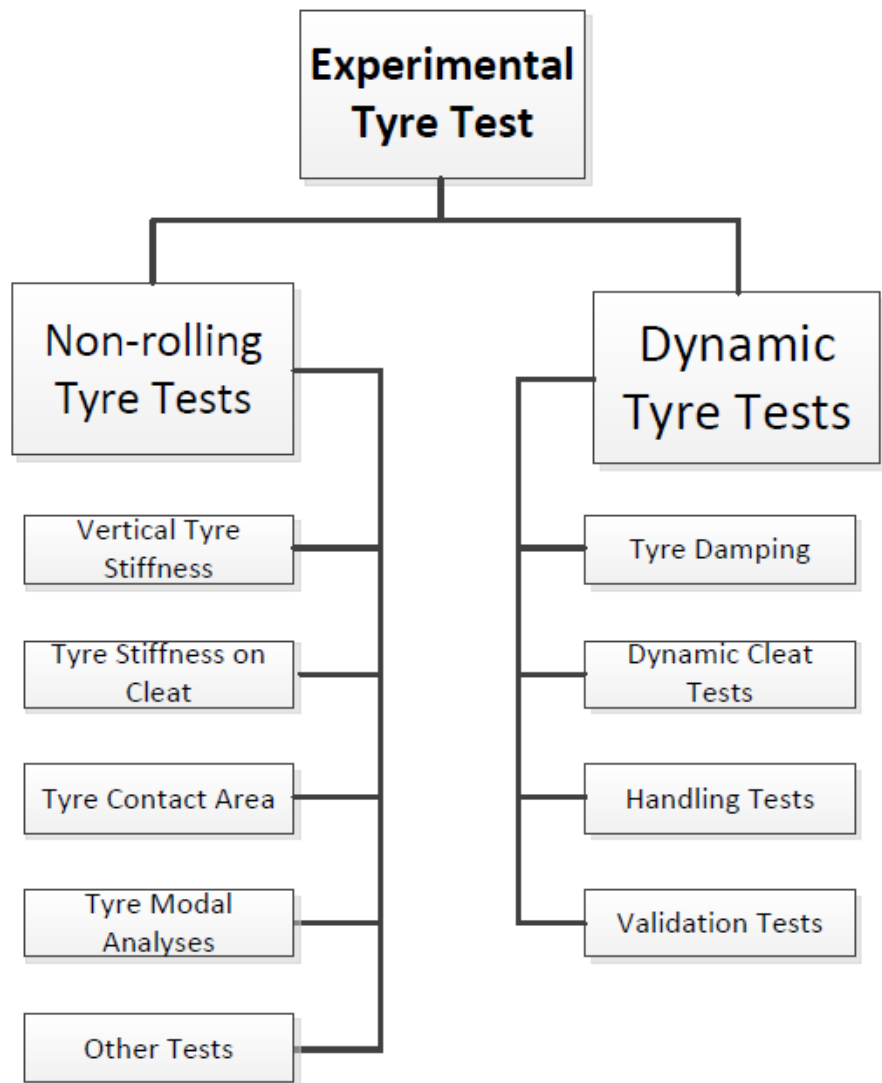


Figure 1

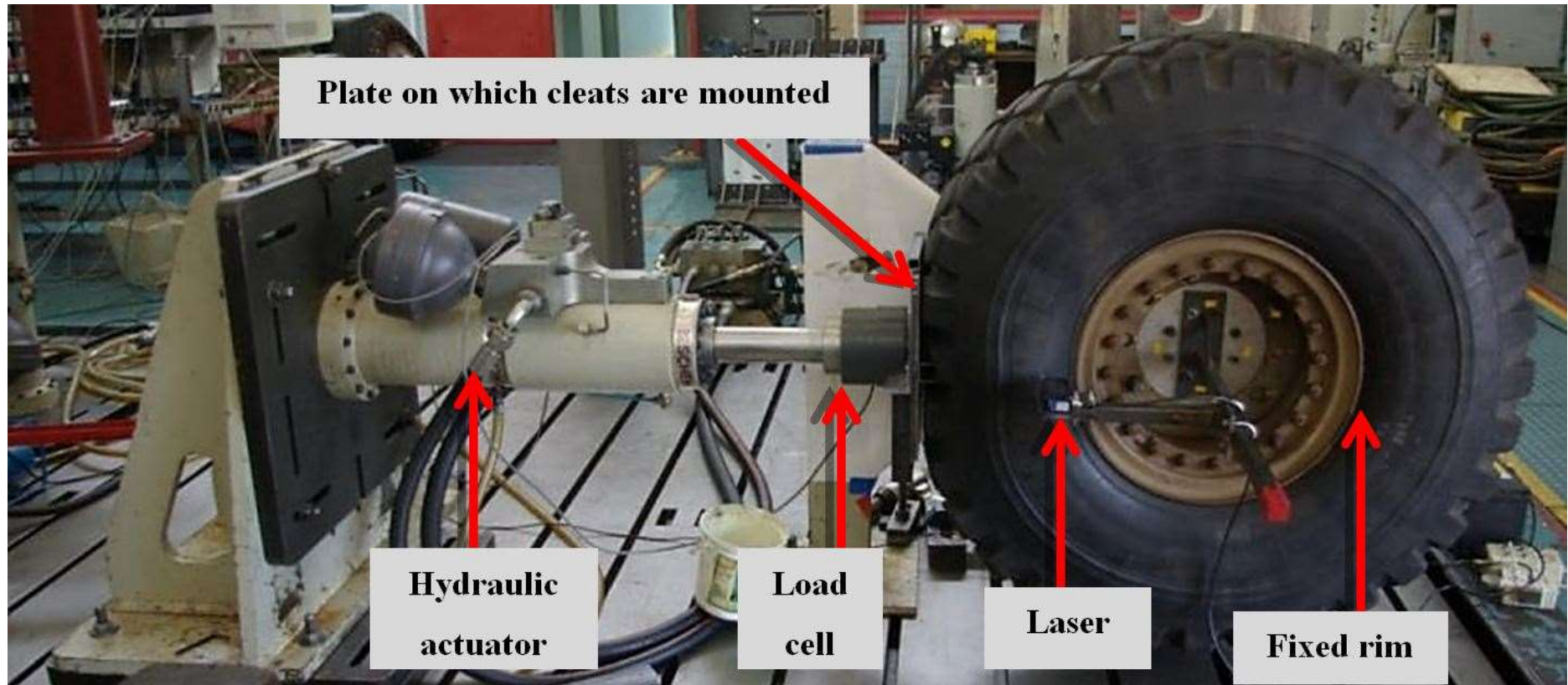


Figure 2

Applied Load vs displacement

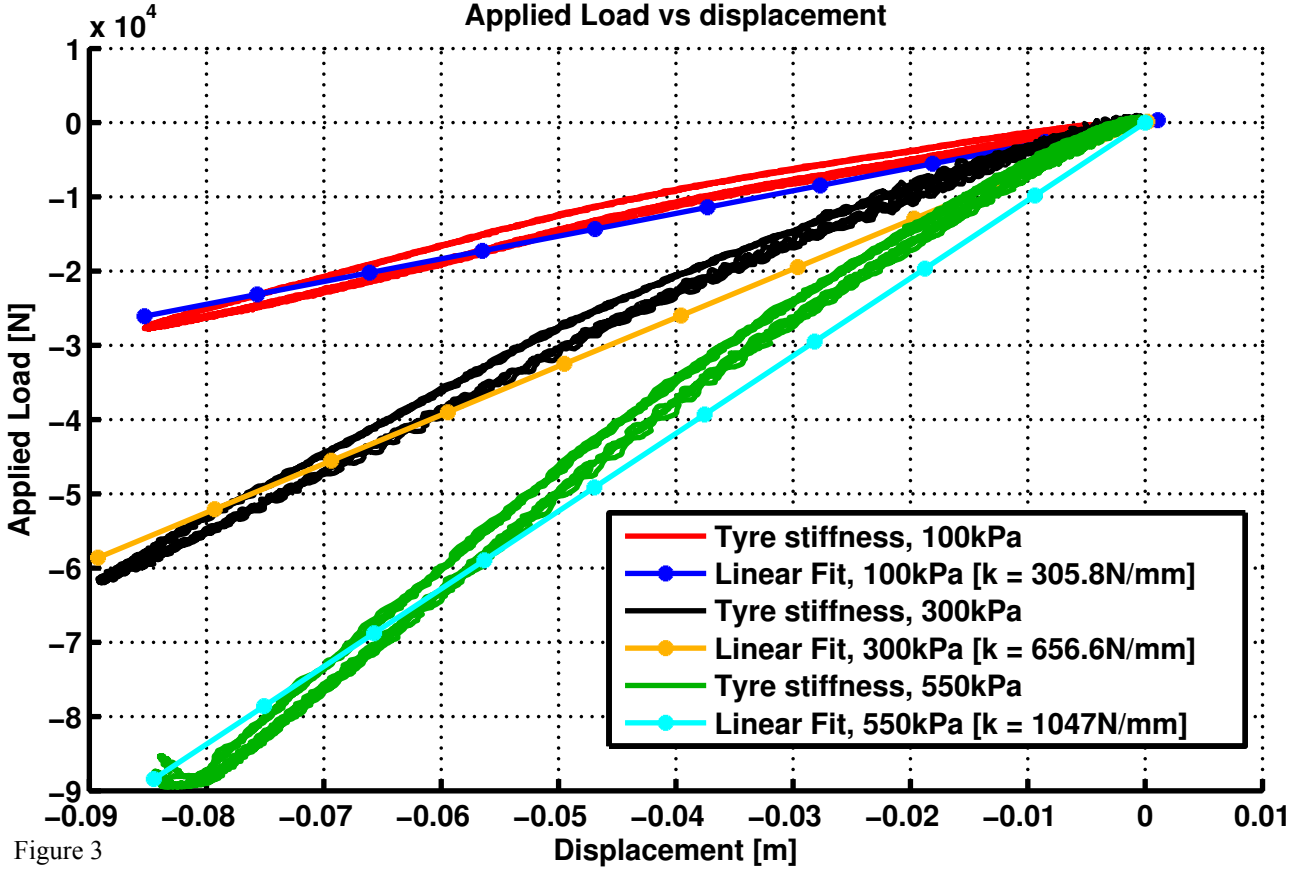


Figure 3

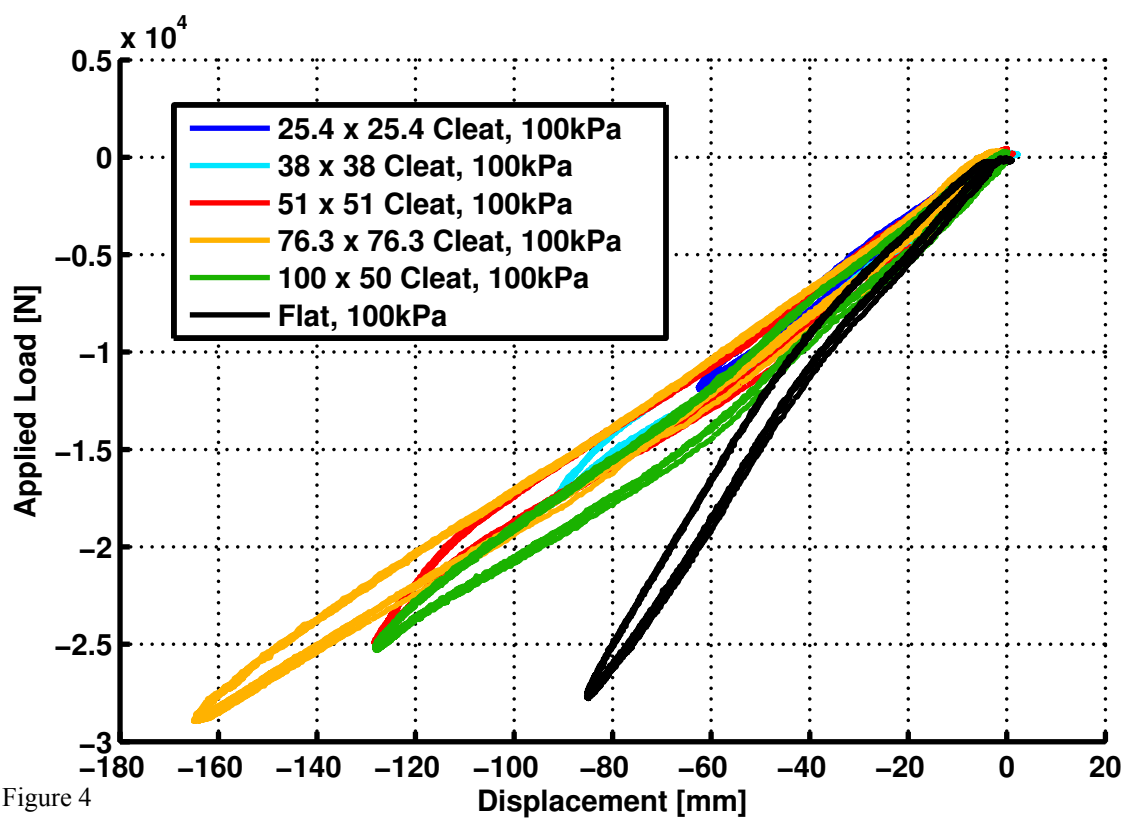


Figure 4

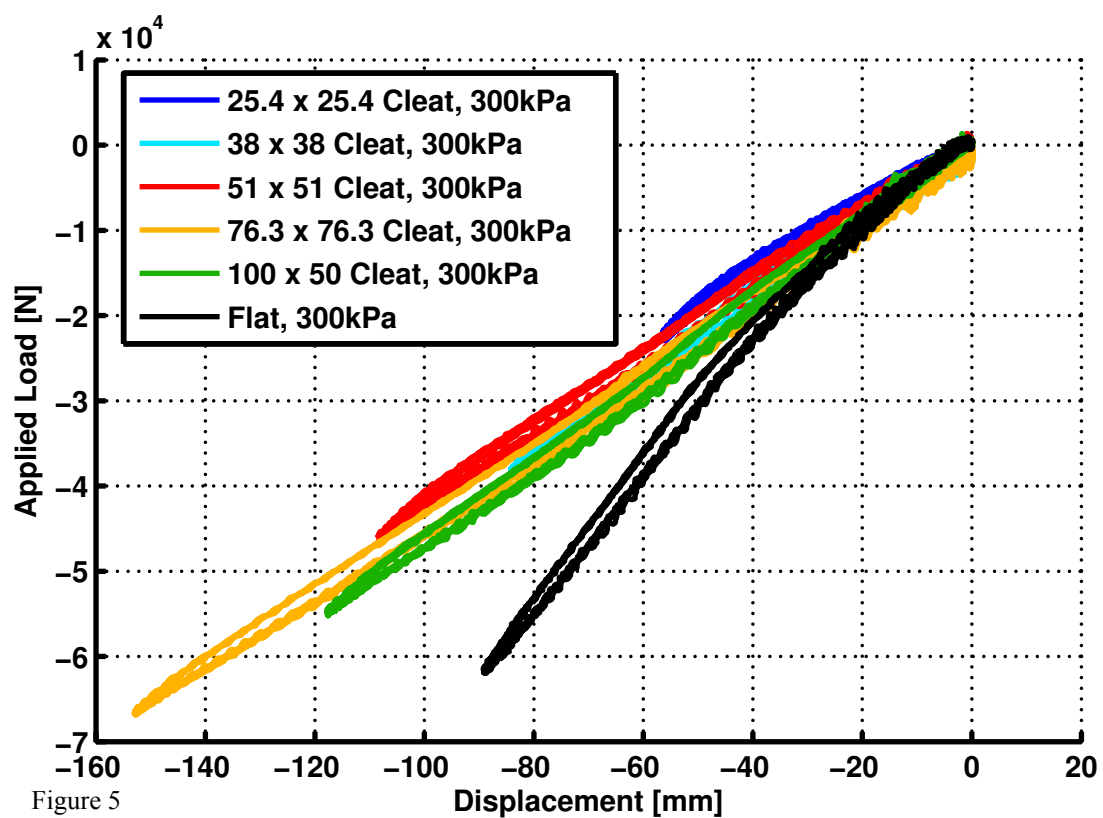


Figure 5

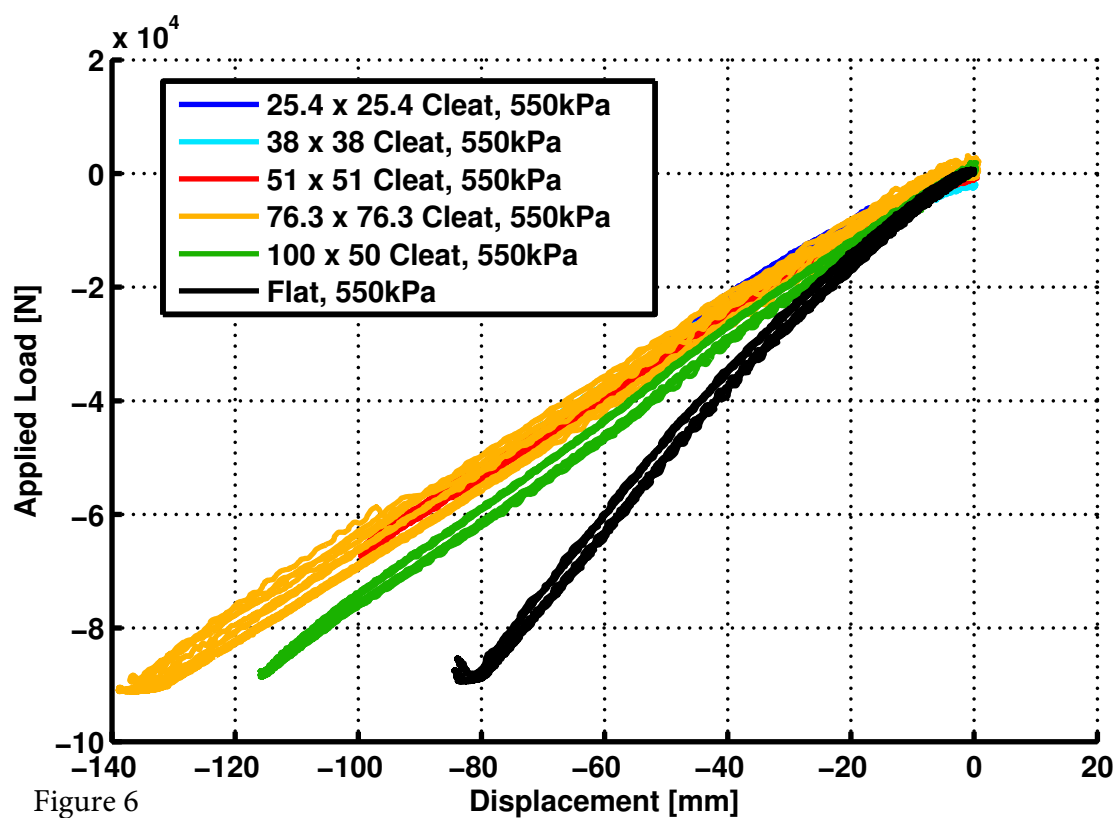


Figure 6

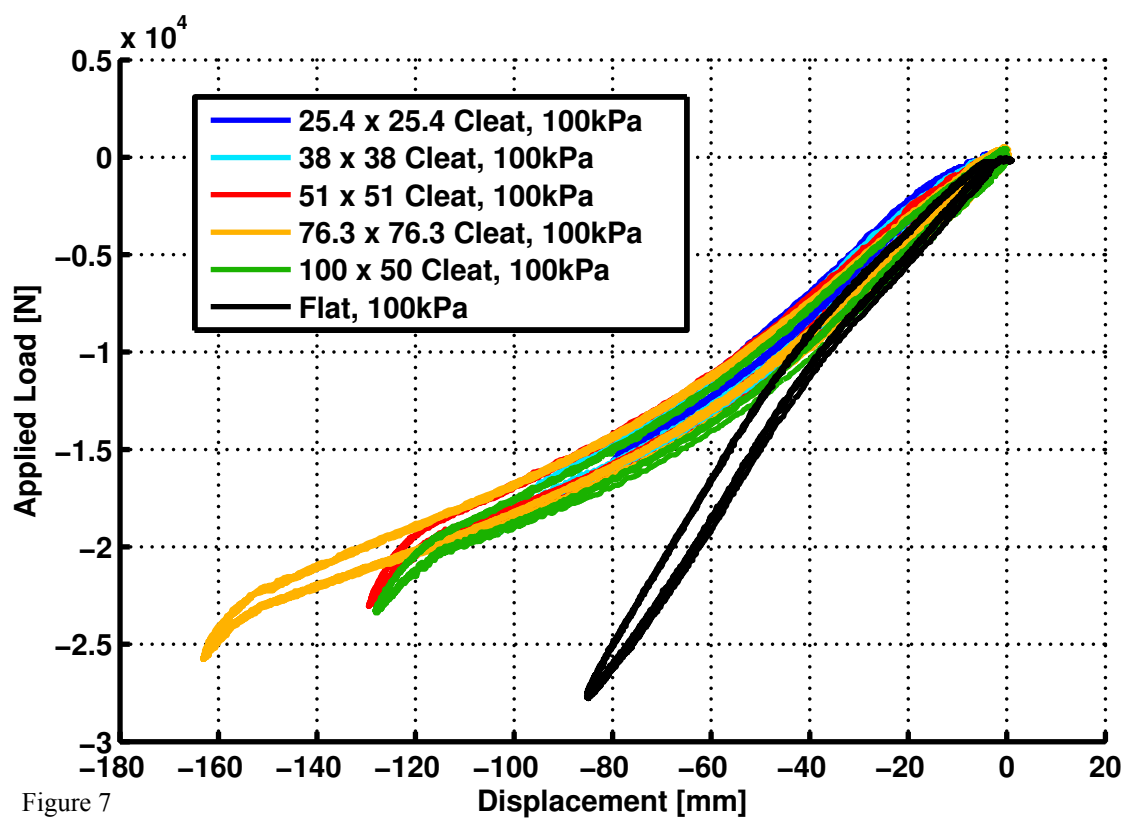


Figure 7

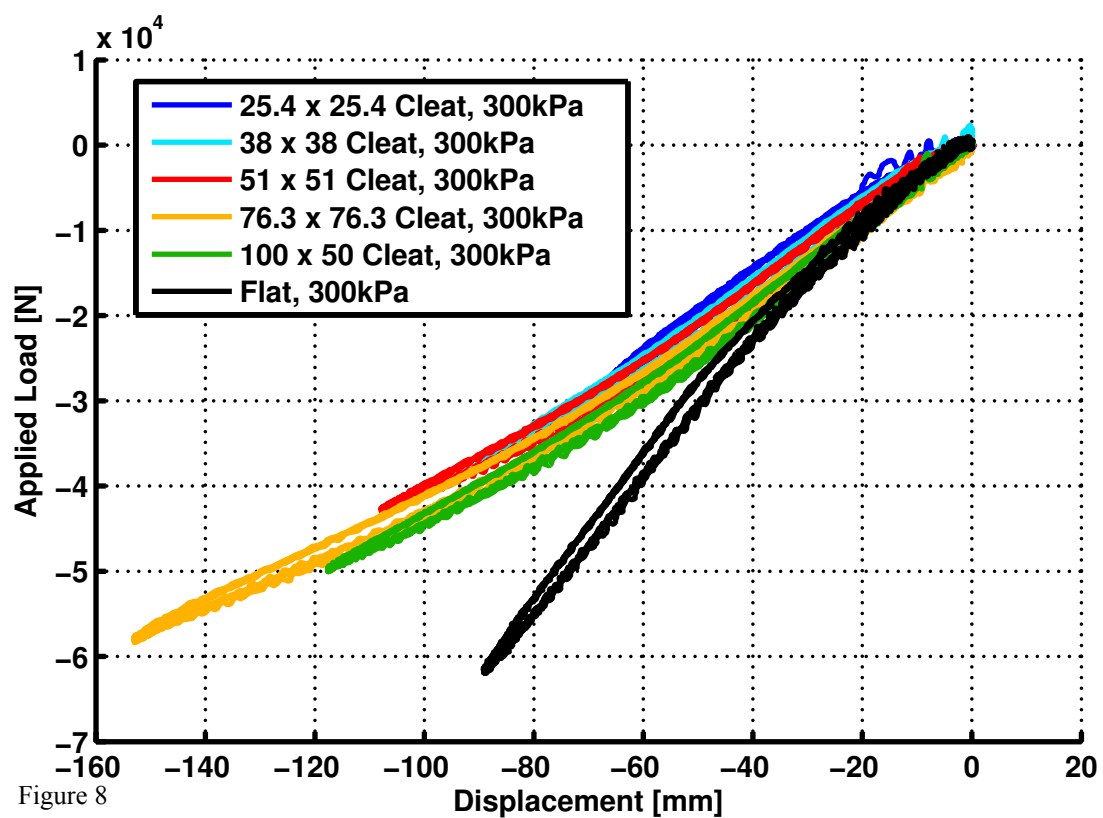


Figure 8

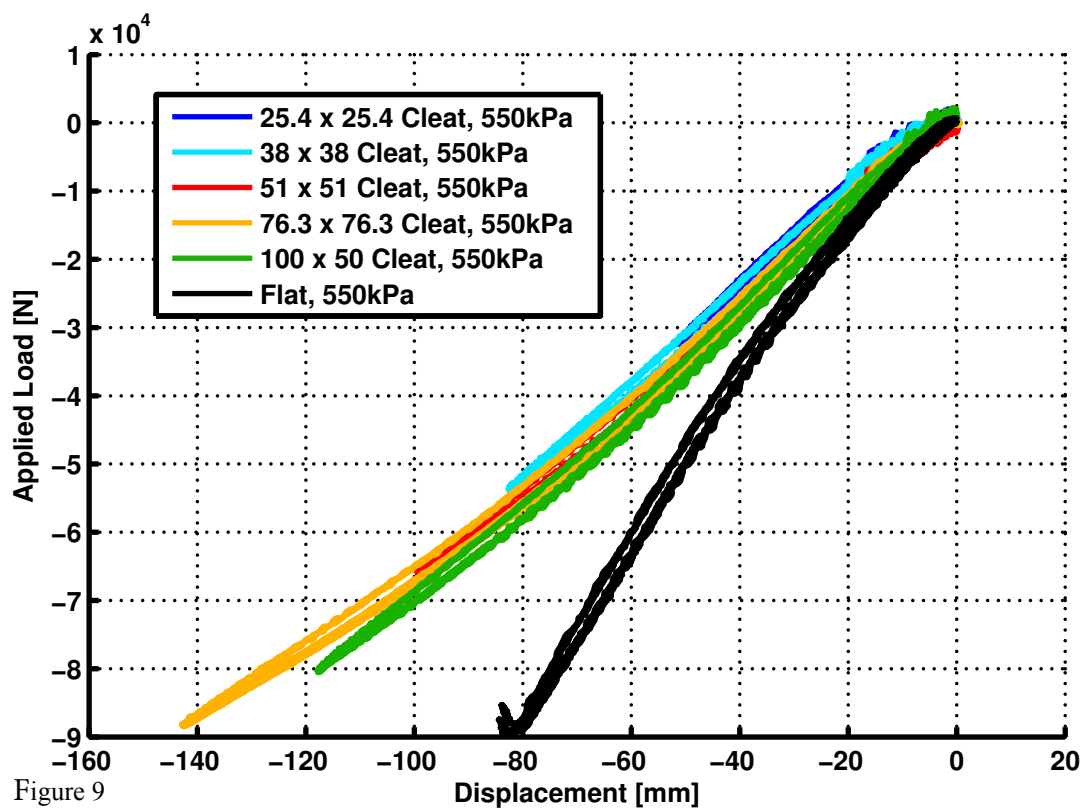


Figure 9

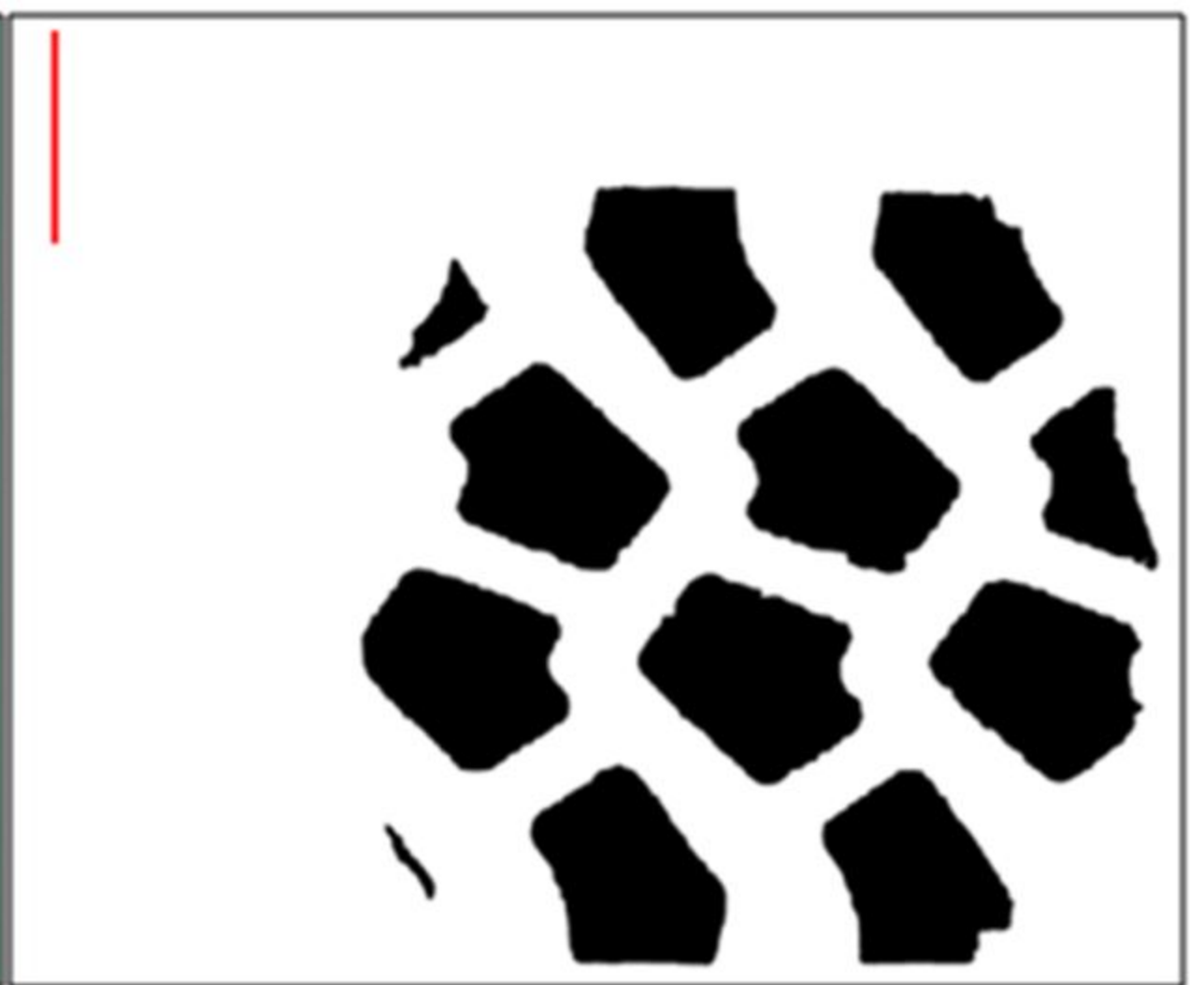
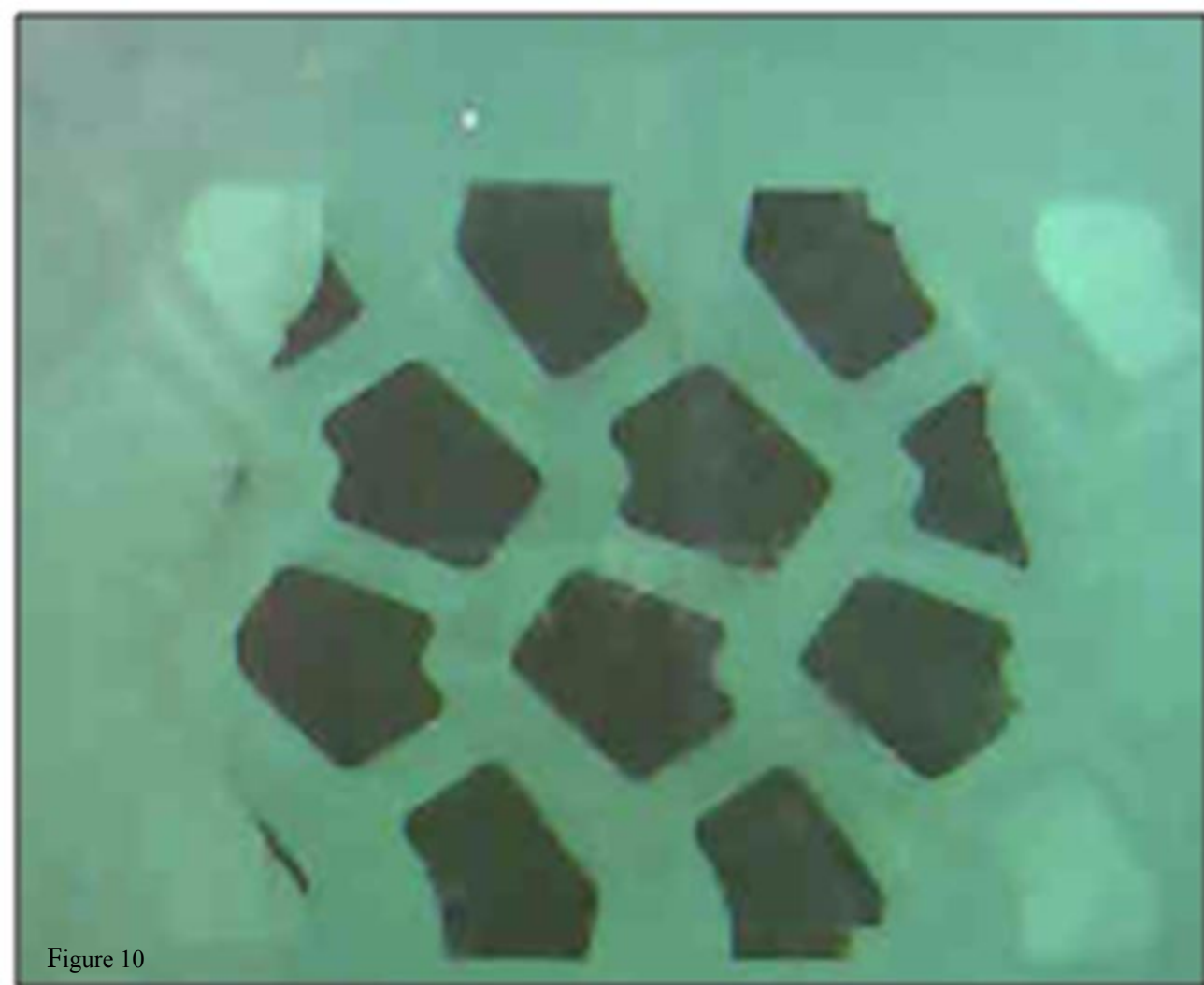
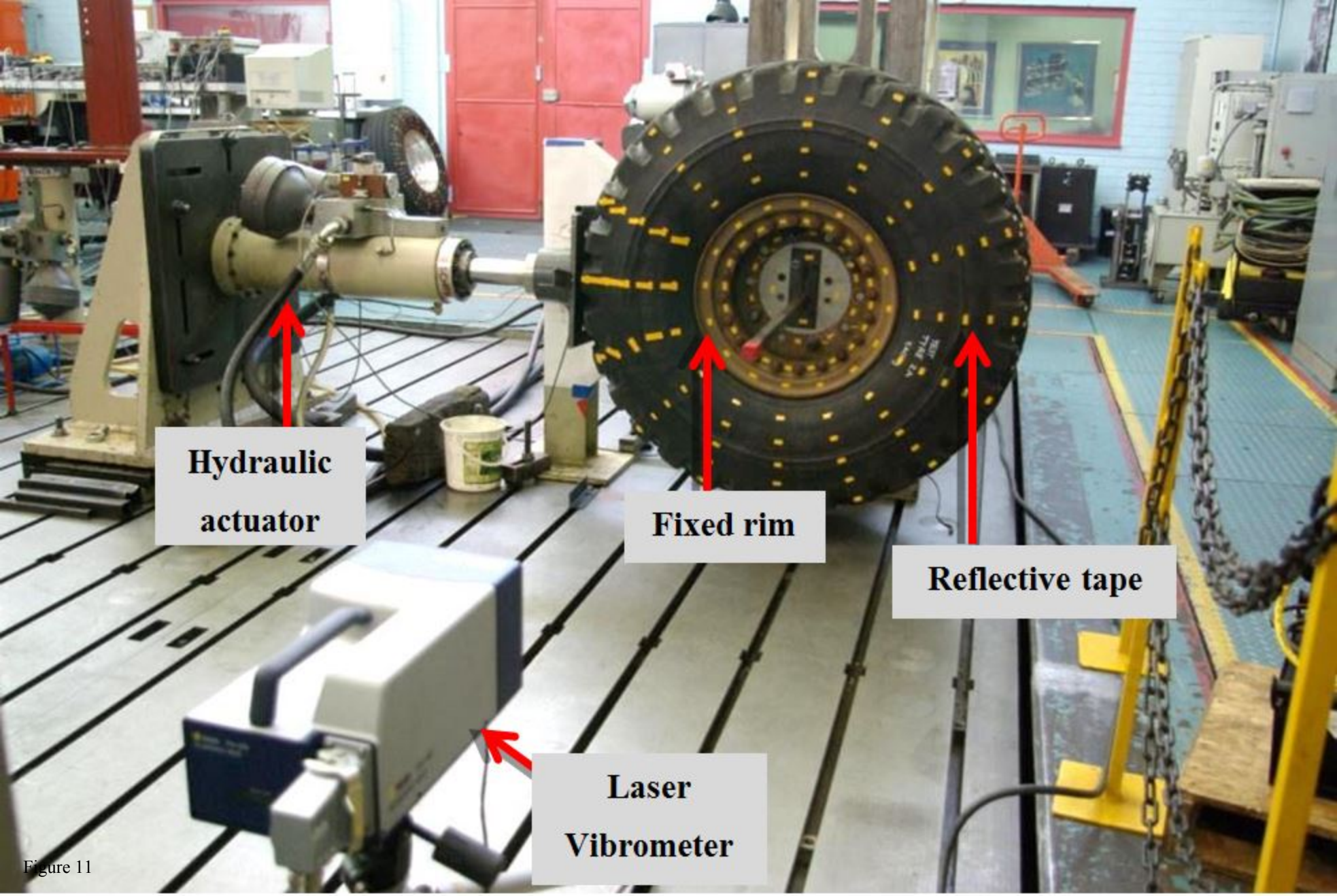


Figure 10



**Hydraulic
actuator**

Fixed rim

Reflective tape

**Laser
Vibrometer**

Figure 11

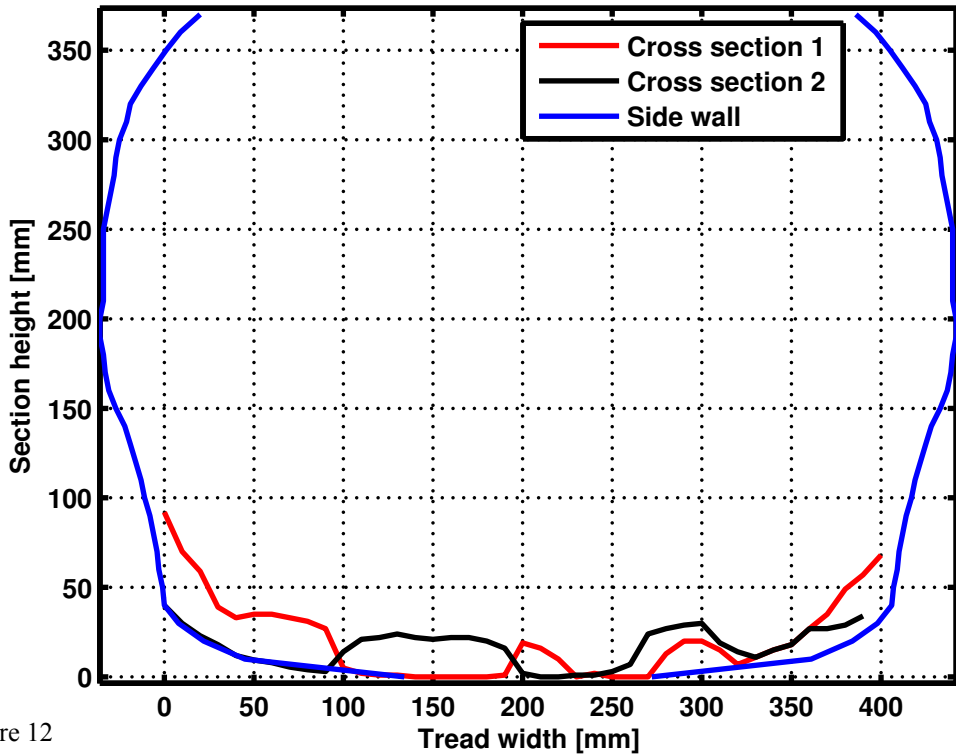


Figure 12



Figure 13

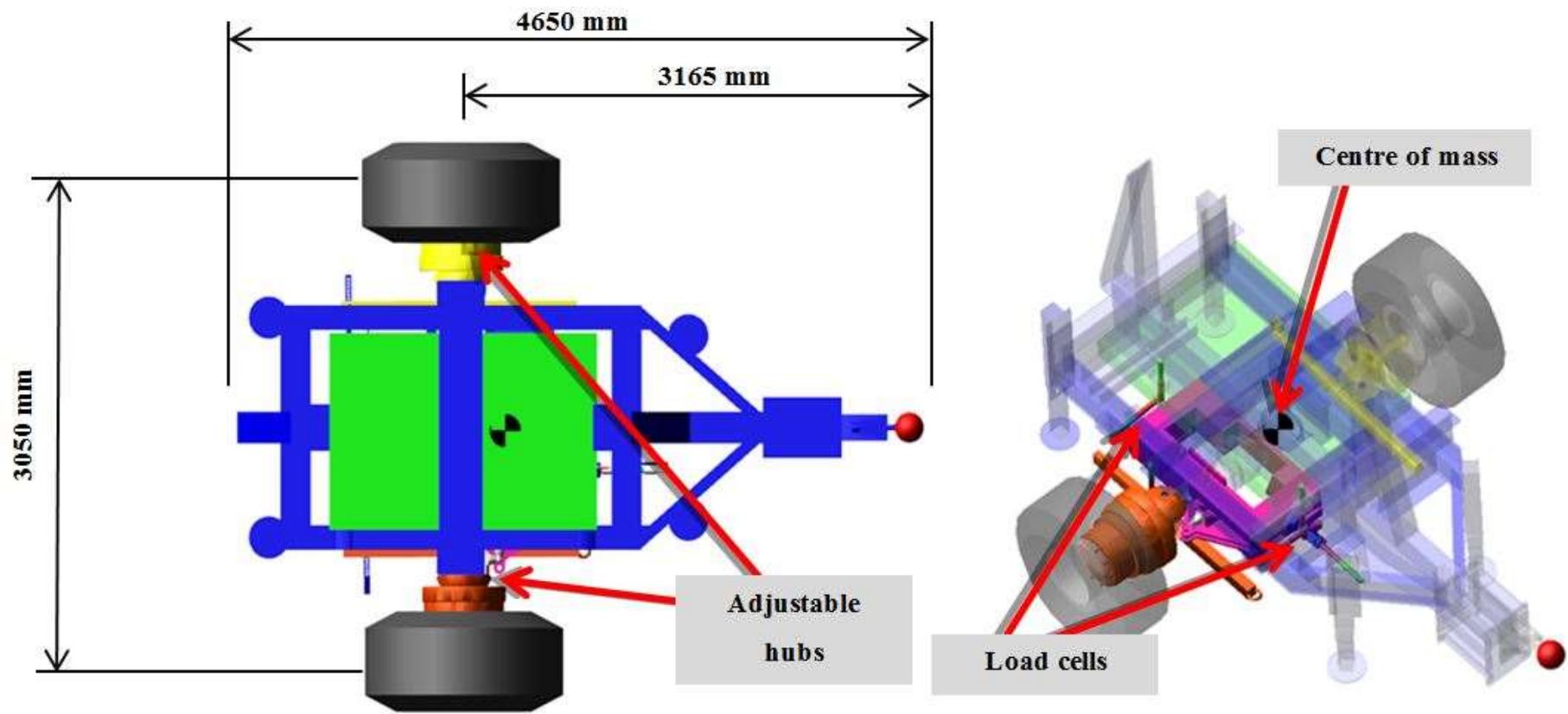


Figure 14

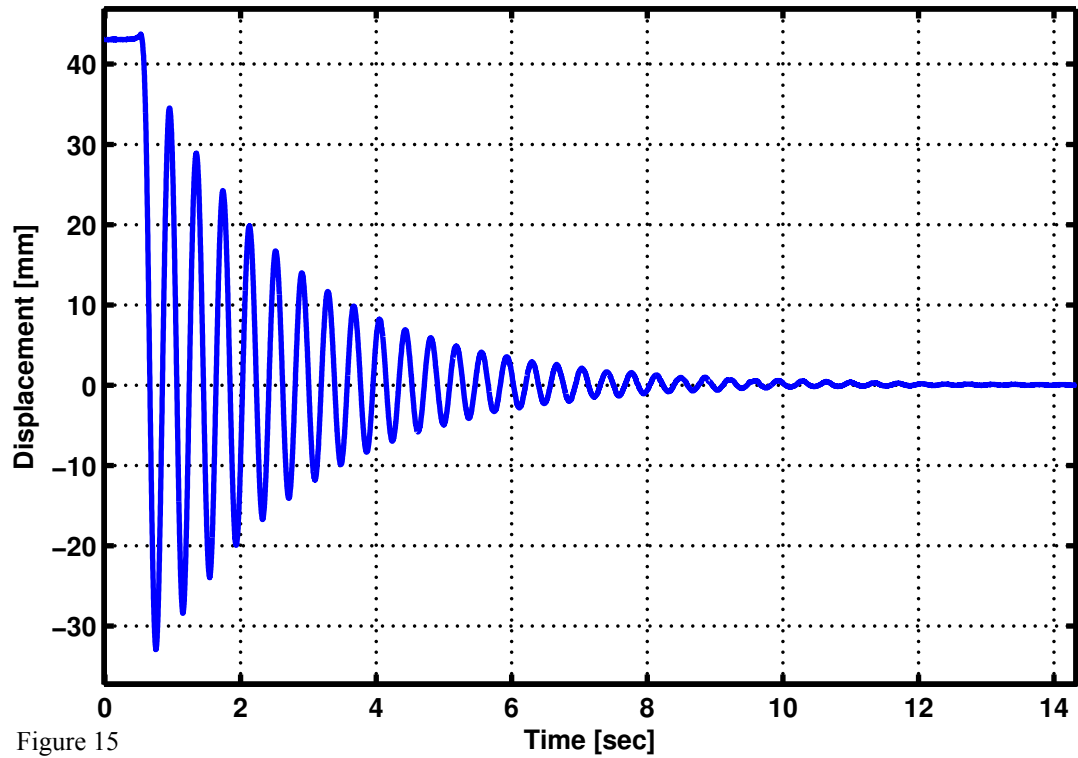


Figure 15

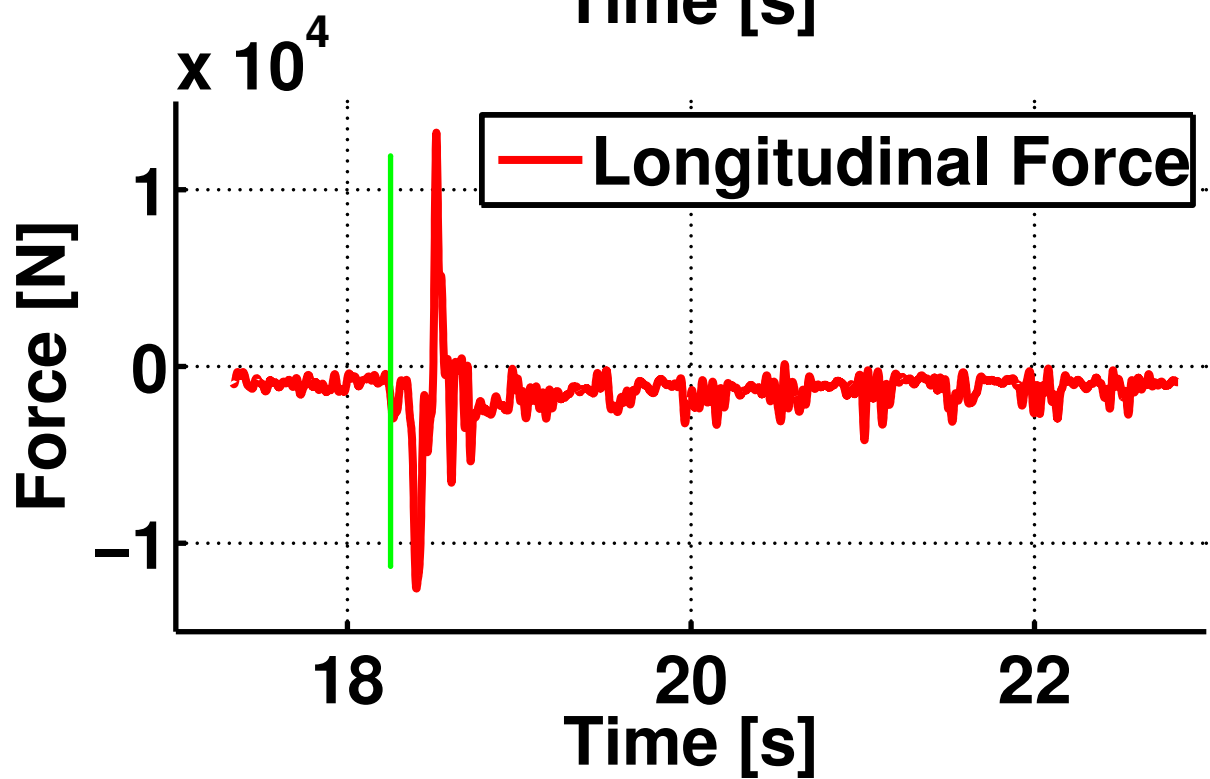
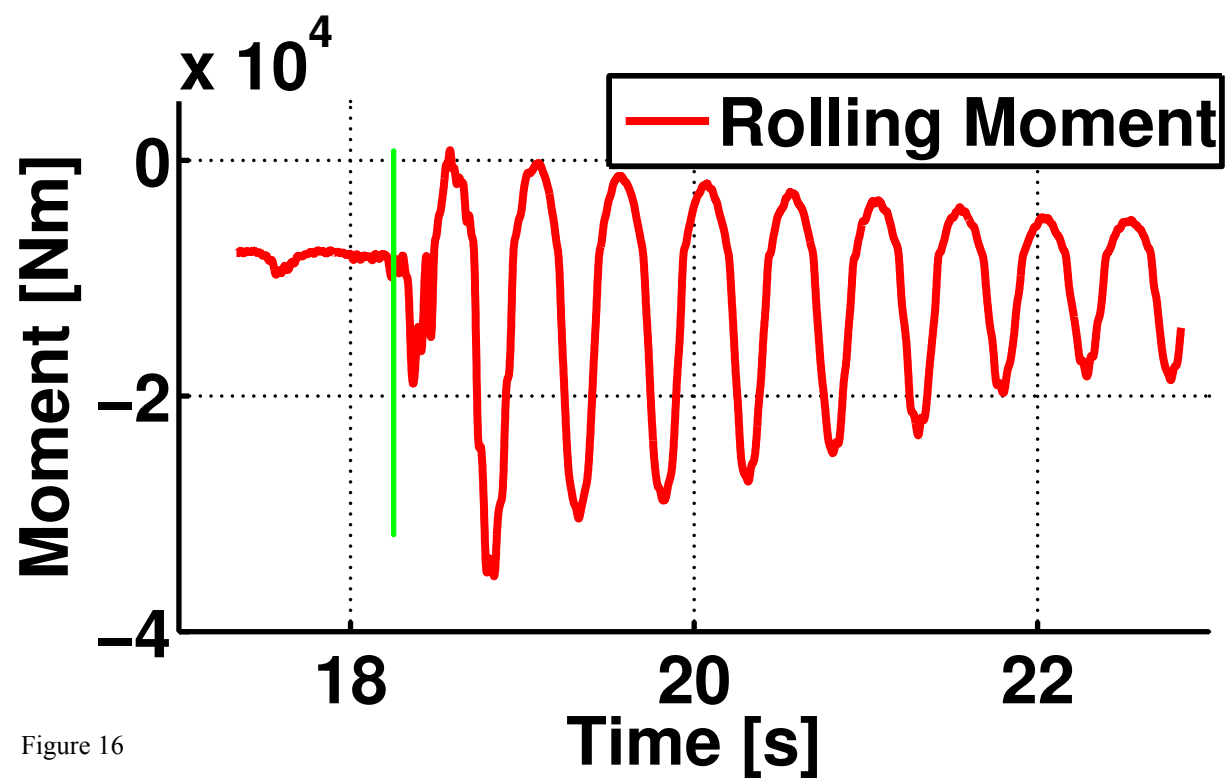
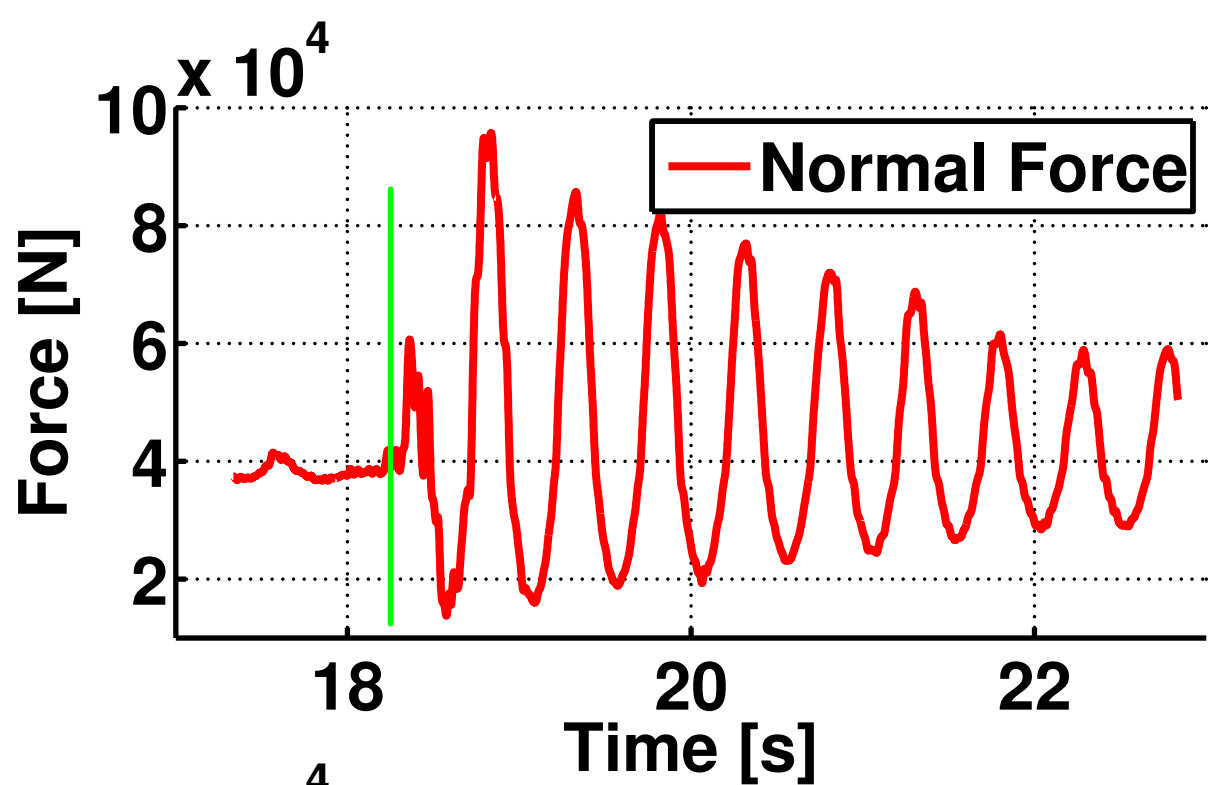


Figure 16

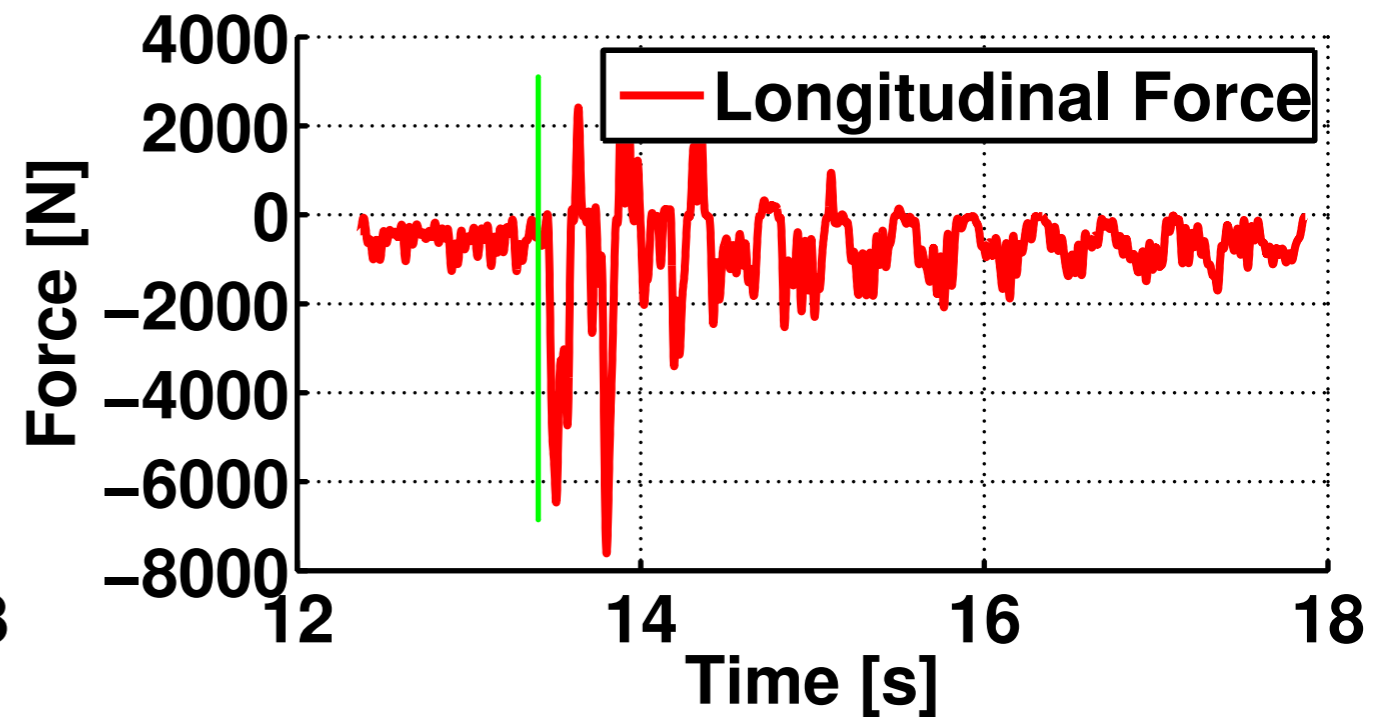
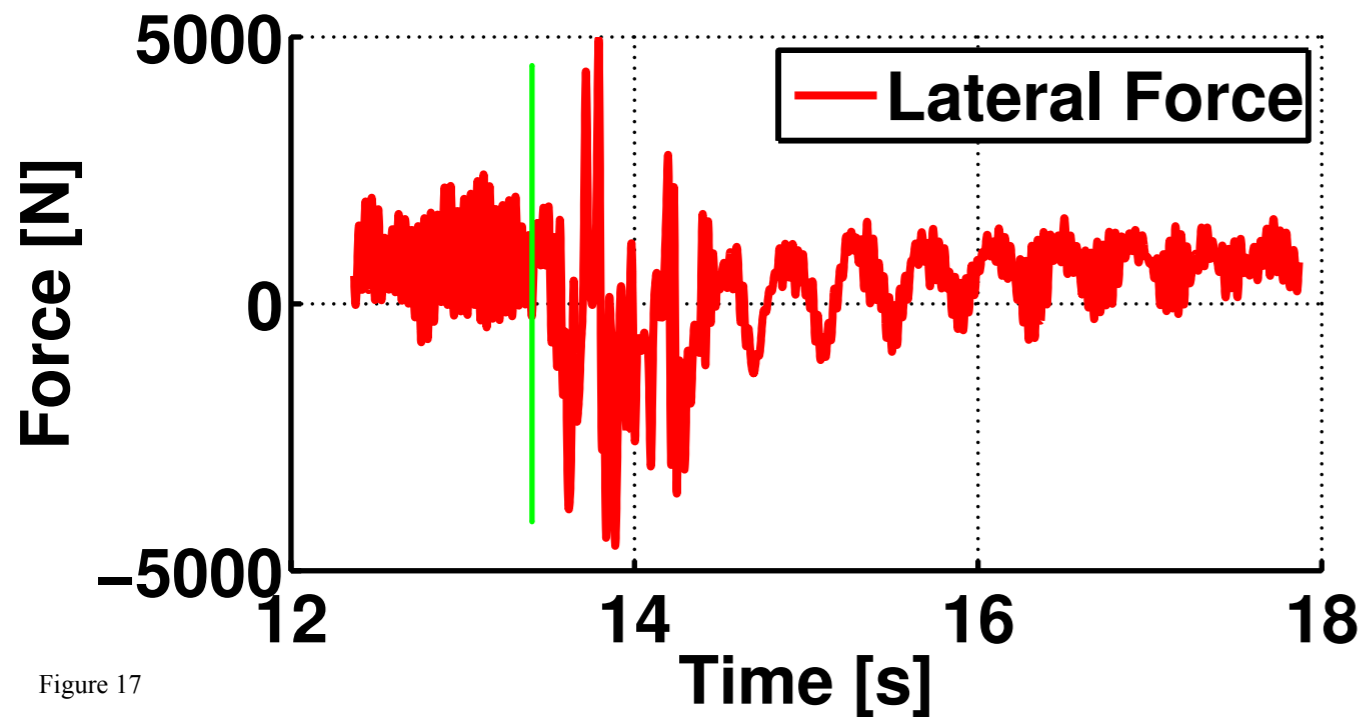
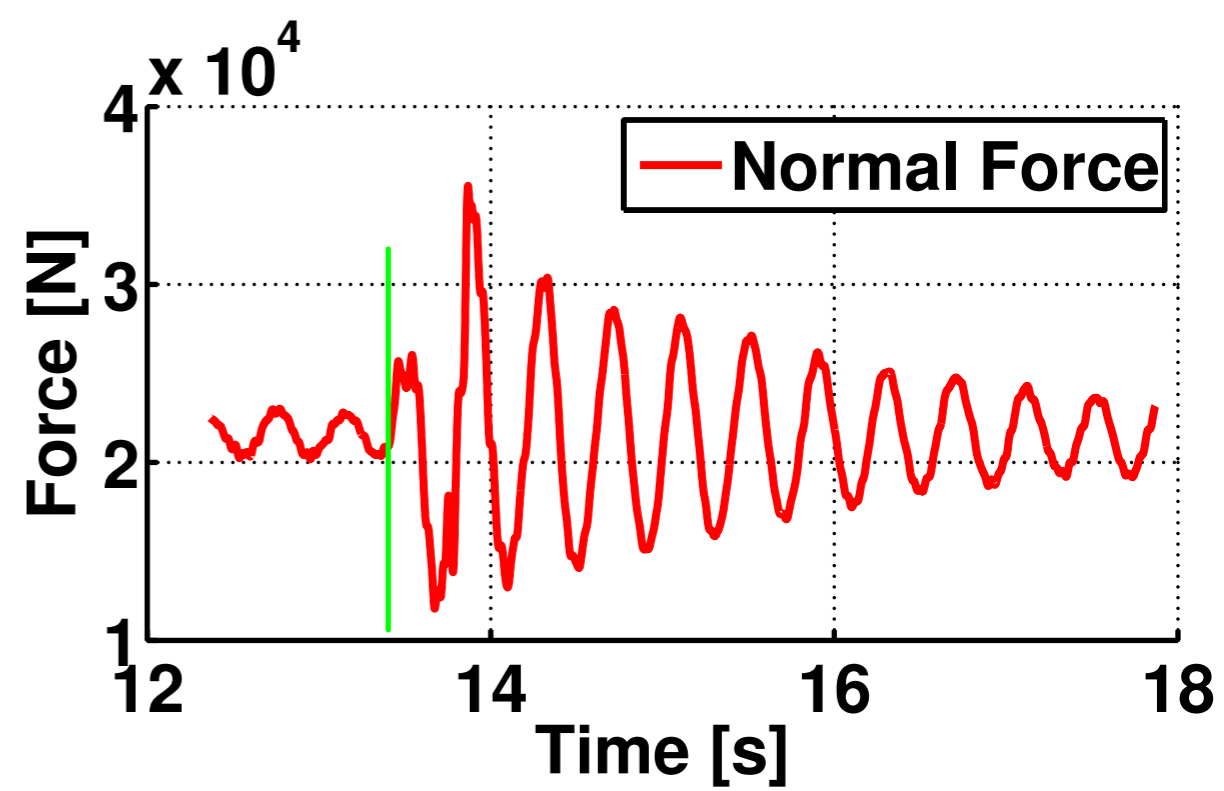


Figure 17

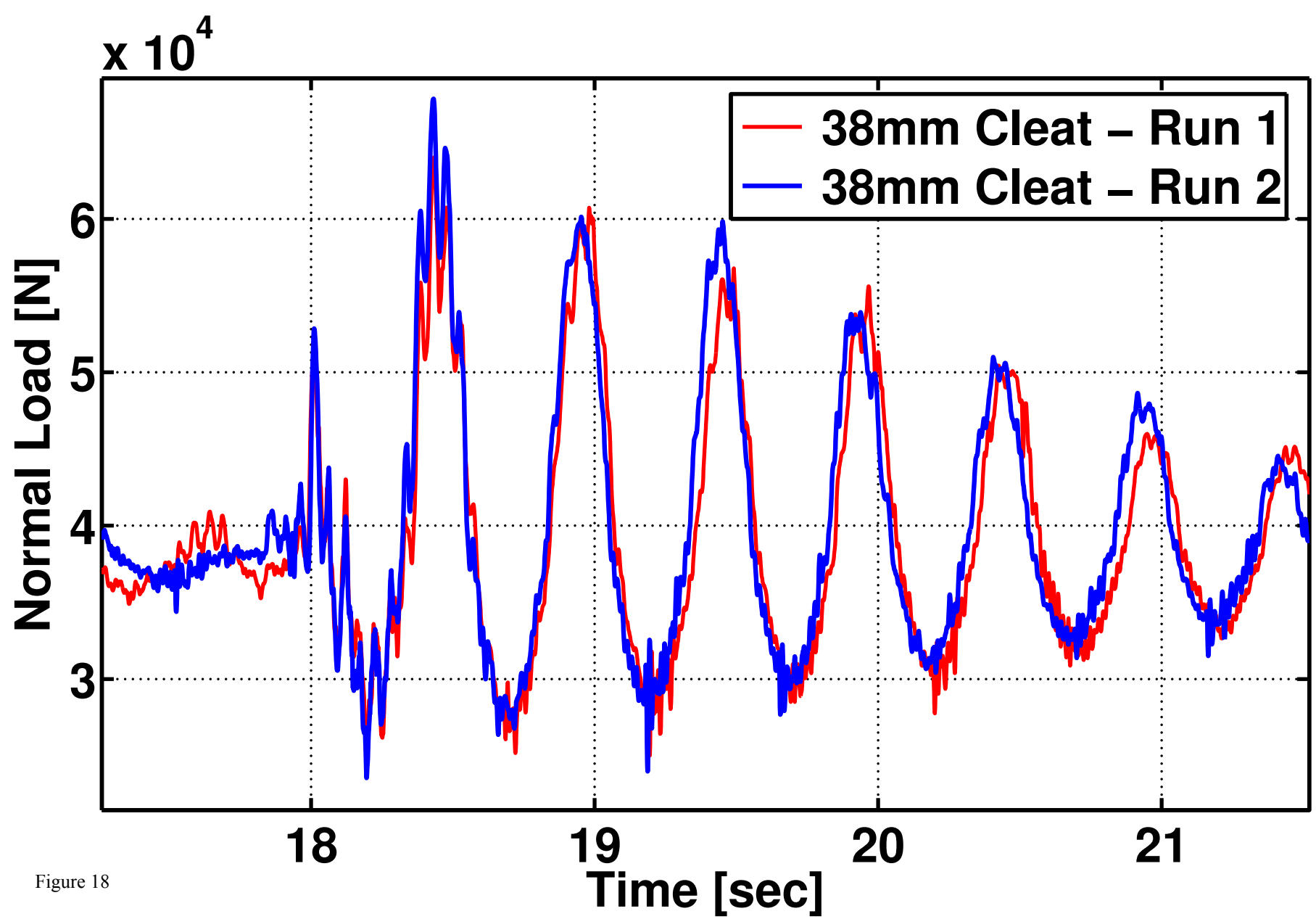


Figure 18

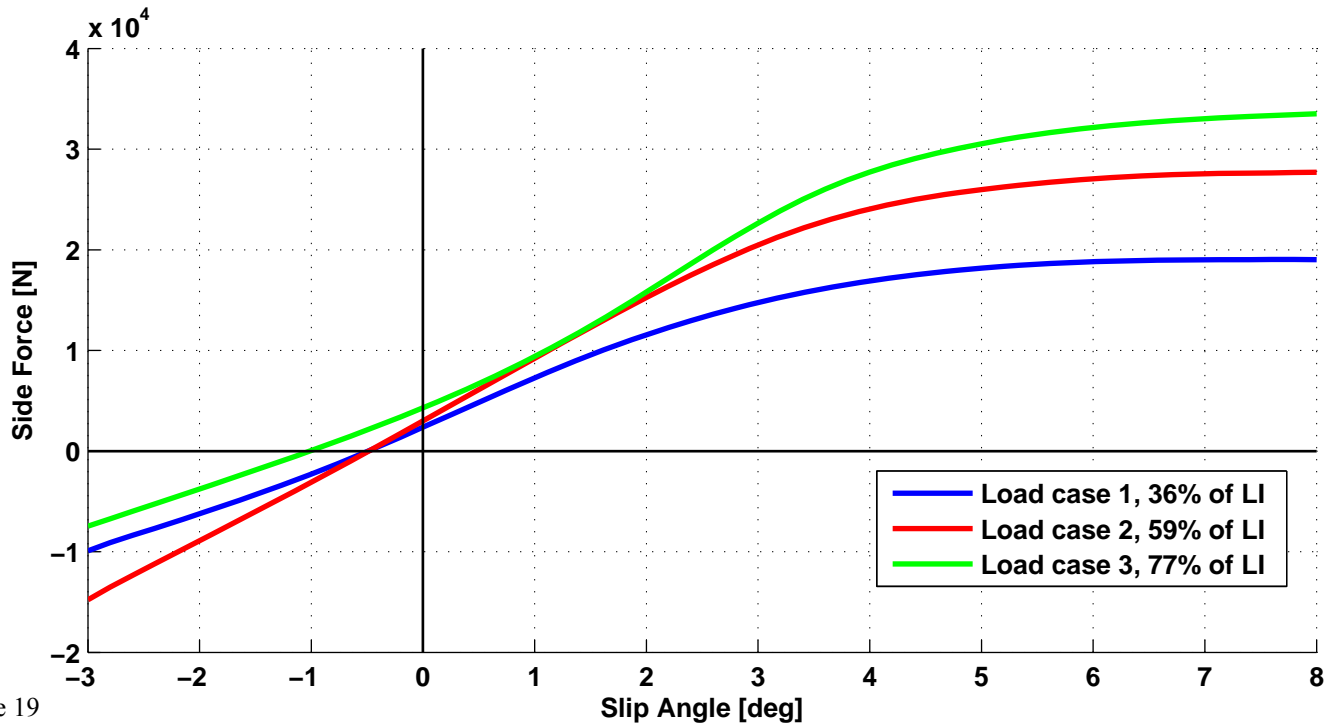


Figure 19

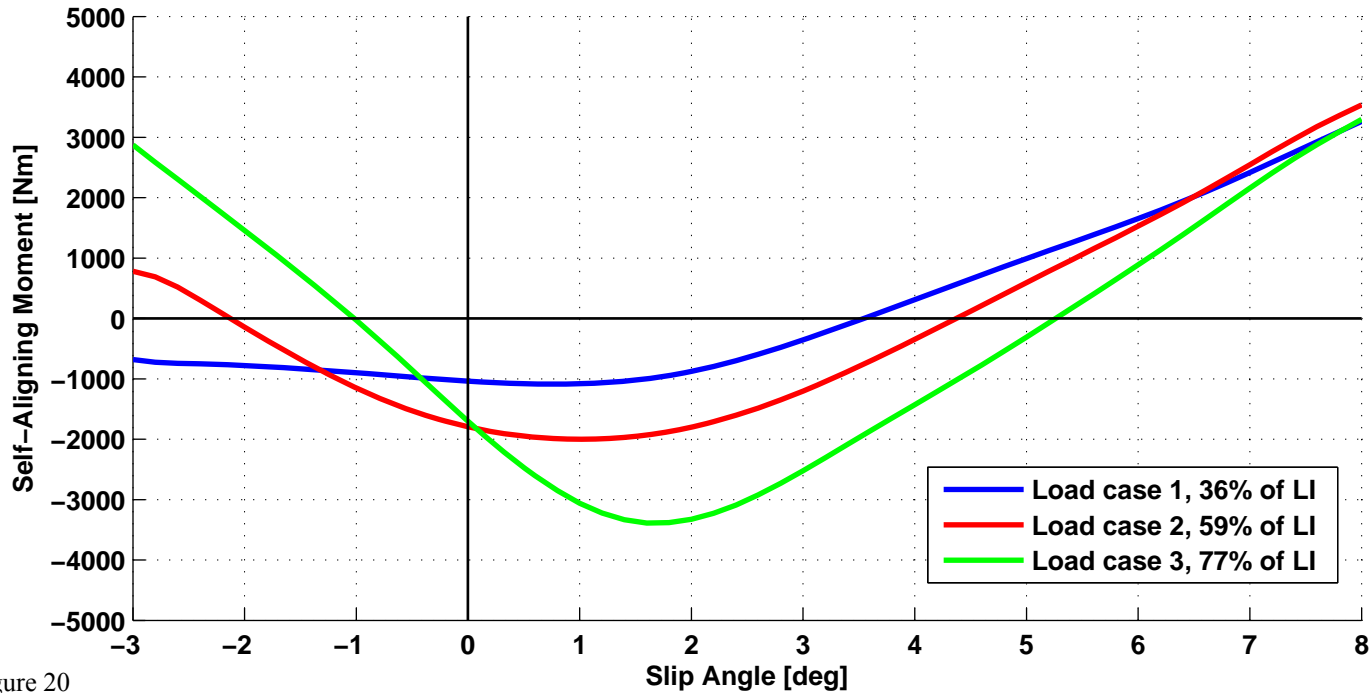


Figure 20

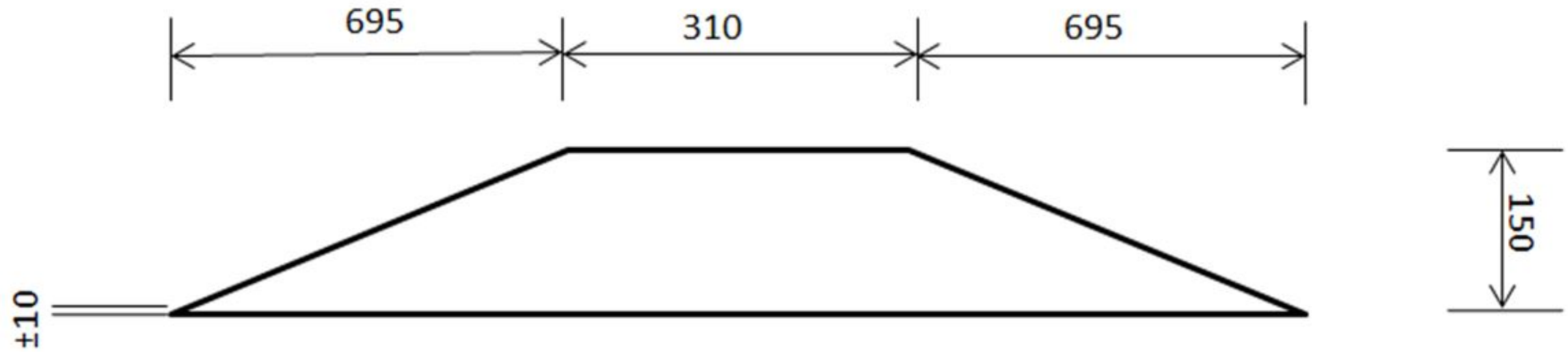


Figure 21

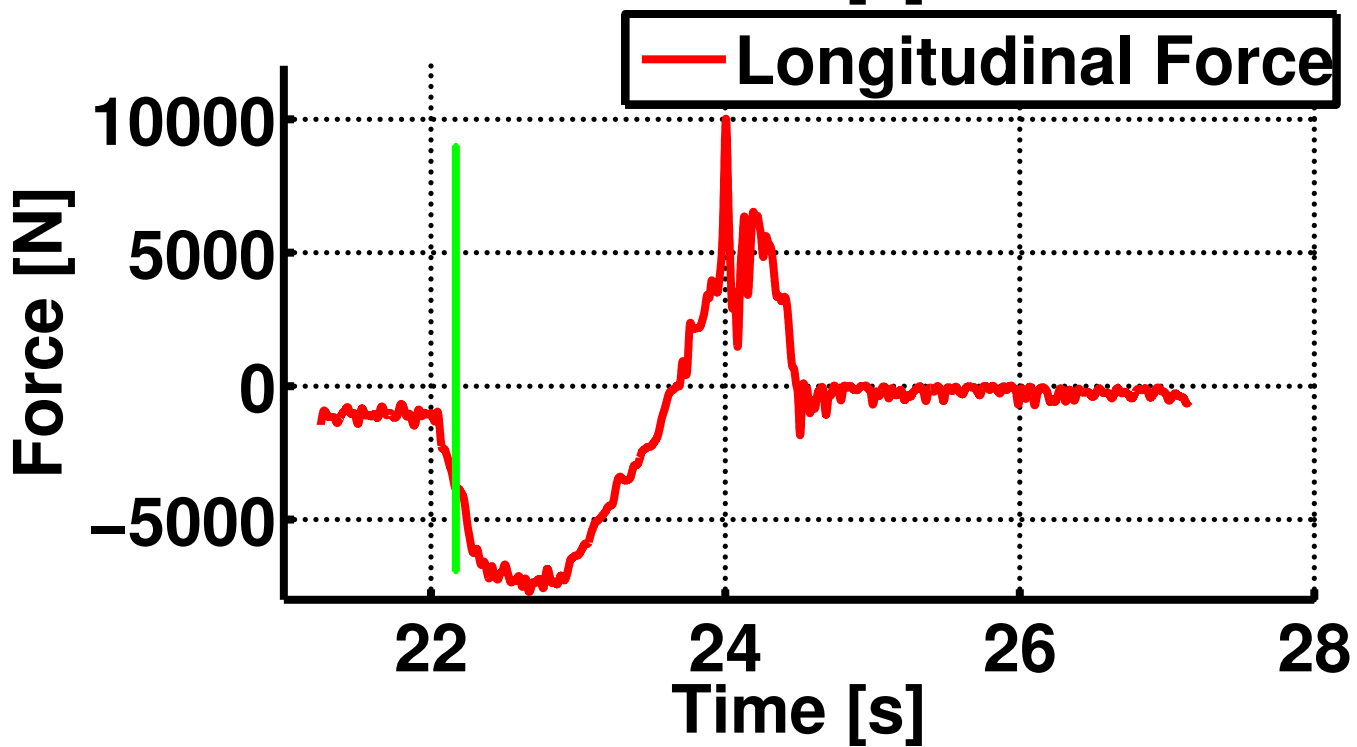
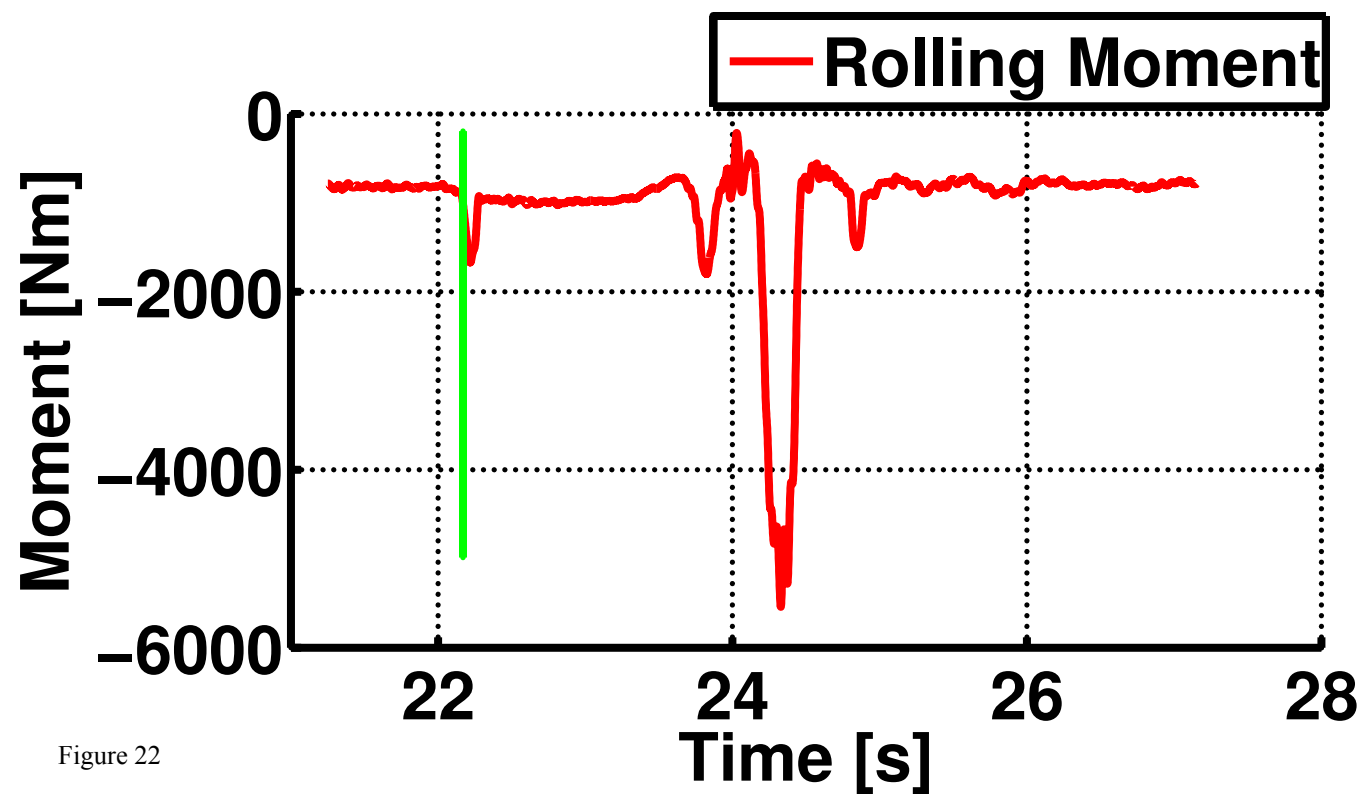
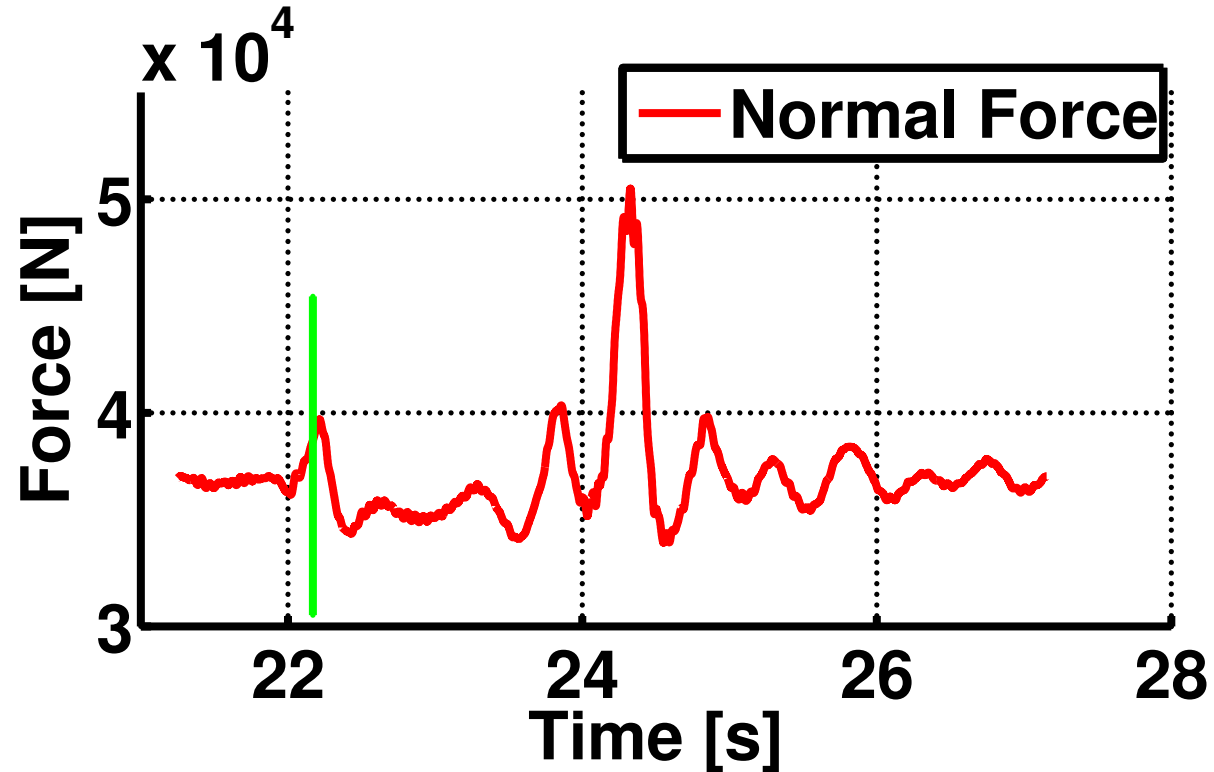


Figure 22

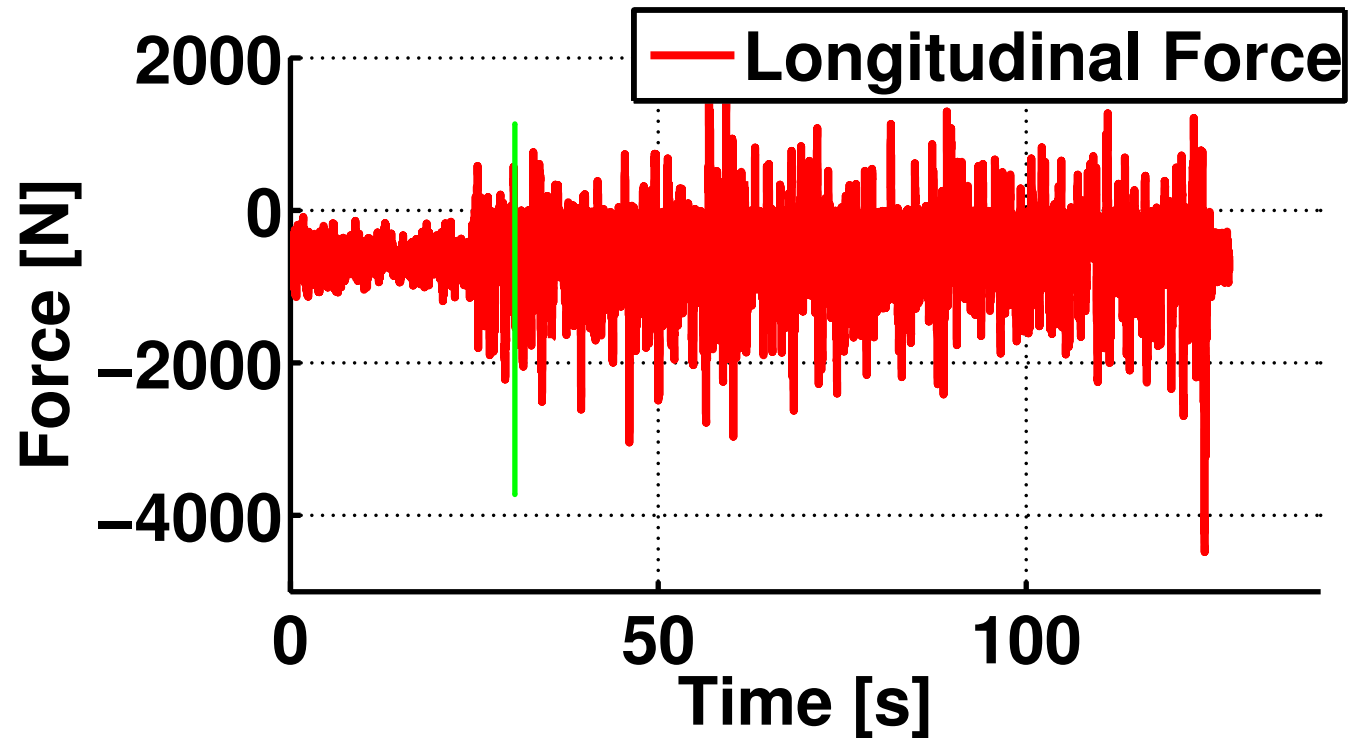
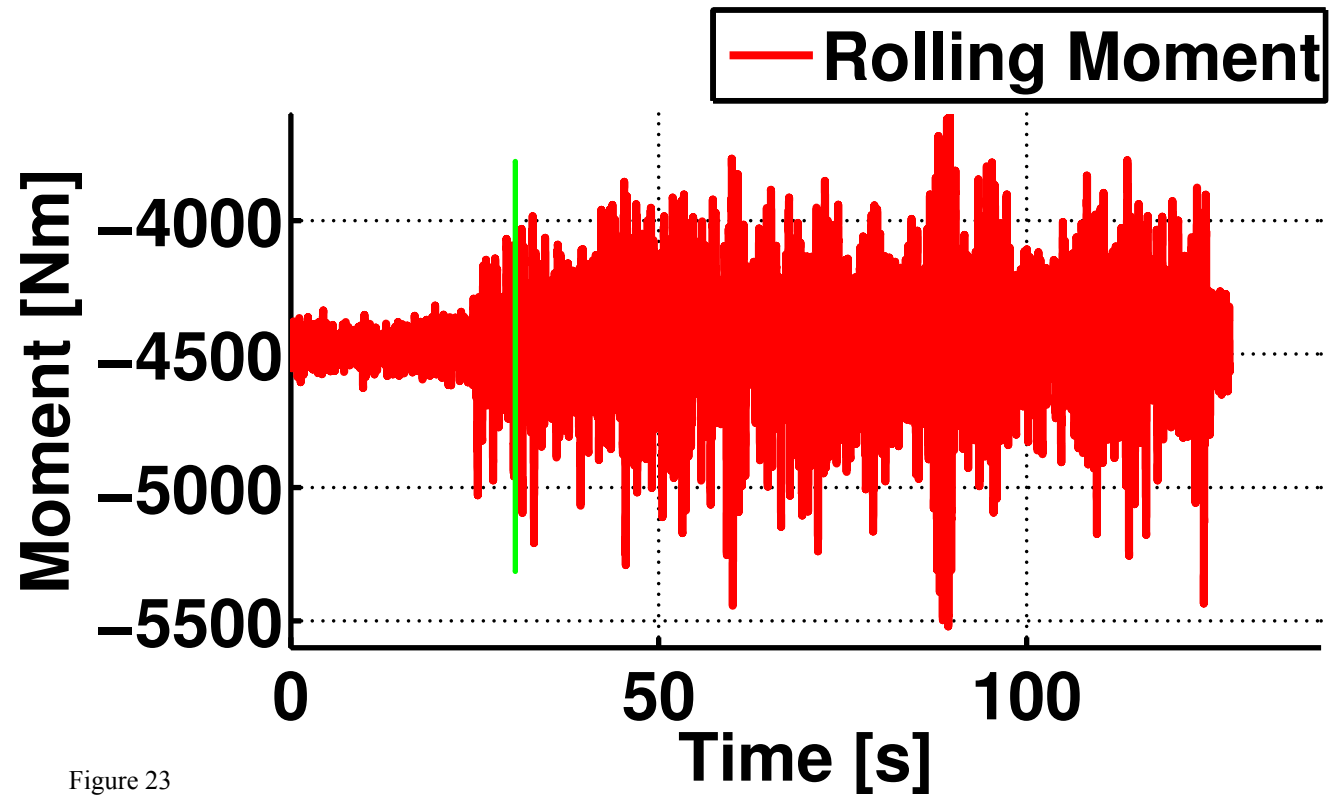
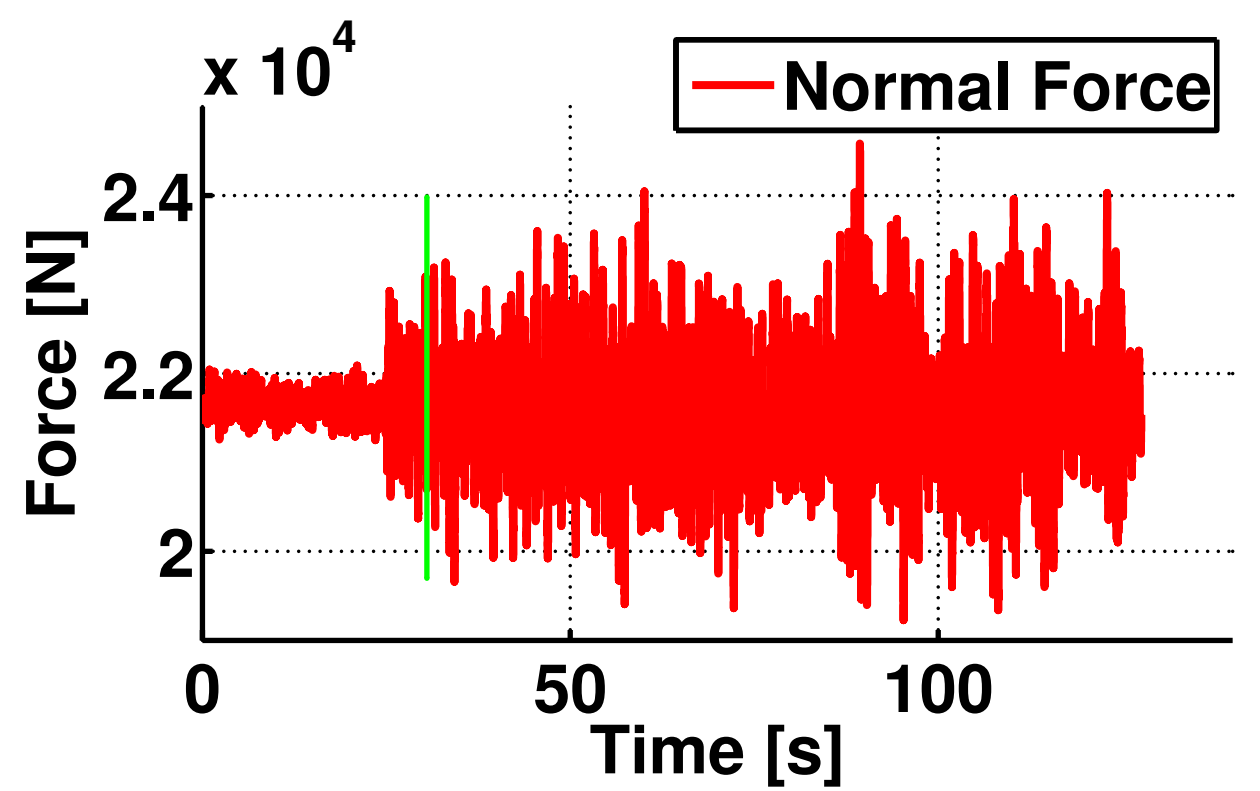


Figure 23